



HAL
open science

Bi-decadal changes in nutrient concentrations and ratios in marine coastal ecosystems: The case of the Arcachon bay, France

A. Lheureux, V. David, Y. del Amo, D. Soudant, I. Auby, F. Ganthy, H. Blanchet, M. -A. Cordier, L. Costes, S. Ferreira, et al.

► To cite this version:

A. Lheureux, V. David, Y. del Amo, D. Soudant, I. Auby, et al.. Bi-decadal changes in nutrient concentrations and ratios in marine coastal ecosystems: The case of the Arcachon bay, France. *Progress in Oceanography*, 2022, 201, 10.1016/j.pocean.2022.102740 . insu-03678659

HAL Id: insu-03678659

<https://insu.hal.science/insu-03678659>

Submitted on 22 Jul 2024

HAL is a multi-disciplinary open access archive for the deposit and dissemination of scientific research documents, whether they are published or not. The documents may come from teaching and research institutions in France or abroad, or from public or private research centers.

L'archive ouverte pluridisciplinaire **HAL**, est destinée au dépôt et à la diffusion de documents scientifiques de niveau recherche, publiés ou non, émanant des établissements d'enseignement et de recherche français ou étrangers, des laboratoires publics ou privés.



Distributed under a Creative Commons Attribution - NonCommercial 4.0 International License

1 Bi-decadal changes in nutrient concentrations and ratios in
2 marine coastal ecosystems: the case of the Arcachon bay,
3 France.

4

5 Authors: Lheureux A. (1)*, David V. (1), Del Amo Y. (1), Soudant D. (2), Auby I. (4), Ganthy
6 F. (4), Blanchet H. (1), Cordier M-A. (1), Costes L. (1), Ferreira S. (1), Mornet L. (1),
7 Nowaczyk A. (1), Parra M. (1), D'Amico F. (4), Gouriou L. (4), Meteigner C. (4), Oger-
8 Jeanneret H. (4), Rigouin L. (4), Rumebe M. (4), Tournaire M-P. (4), Trut F. (4), Trut G. (4),
9 Savoye N. (1).

10 *Corresponding author: arnaud.lheureux@u-bordeaux.fr; Station Marine d'Arcachon, 2 rue
11 du Professeur Jolyet, 33120 Arcachon, France.

12

13 (1) Université de Bordeaux-CNRS, UMR 5805, Environnement Paléoenvironnement
14 Océaniques et Côtiers (EPOC), 2 Rue du Professeur Jolyet, 33120 Arcachon, France.

15 (2) Ifremer Nantes, Valorisation de l'Information pour la Gestion Intégrée Et la Surveillance
16 (VIGIES), 44311 Cedex 03, Rue de l'Île d'Yeu, 44980 Nantes, France.

17 (3) Sorbonne Université, MNHN, UNICAEN, UA, CNRS, IRD, UMR 7208, Biologie des
18 Organismes et Écosystèmes Aquatiques (BOREA), 61 rue Buffon, CP 53, 75005 Paris,
19 France

20 (4) Ifremer, LER/AR, 1 Quai du Commandant Silhouette, 33120 Arcachon, France

21

22 Keywords: Nutrients, global change, seagrass regression, coastal ecosystem, Arcachon
23 bay

24

25 Highlights :

26 ● $[\text{NO}_x]$, $[\text{NH}_4^+]$ and $[\text{Si}(\text{OH})_4]$ increased but $[\text{PO}_4^{3-}]$ decreased between 2000 and
27 2019.

28 ● Seagrass meadow decline directly and indirectly explained through

29 ● - reduced nutrient consumption and sediment stabilization,

30 ● - increased phytoplankton biomass with high P-need.

31 ● Increase in temperature and changes in wind conditions also mattered.

32 *Colour should be used for all figures in print.

33

34 Abstract:

35 Large amounts of nutrients have been released to the coastal ecosystems during the 20th
36 century. Since then, management policies have been implemented and these amounts
37 decreased in the economically developed countries. We examined the bi-decadal changes
38 in nutrients (nitrate + nitrite, ammonium, orthophosphate and silicic acid) in the Arcachon
39 bay, a semi-enclosed lagoon that hosts one of the largest but declining seagrass meadow
40 in Europe. Seven sites have been sampled for nutrients and biogeochemical parameters
41 during twenty years at low and/or high tide. In addition, continental and climatic data as well
42 as hydro-climatic indices were used. Dynamic linear models were used to assess the bi-
43 decadal changes in nutrient concentrations and ratios, their seasonality, and the bi-decadal
44 changes of their potential drivers. Partial least square path modeling were used to
45 investigate the relationships between potential abiotic drivers and nutrients. During the
46 study period, the concentration of N and Si nutrients increased whereas the concentration
47 of orthophosphate decreased, leading to deep changes in nutrient ratios. Clear
48 relationships between abiotic drivers (local climate, continental inputs and the bay
49 hydrodynamism) and N, P and Si nutrients were highlighted. However, the bi-decadal
50 change in nutrient concentrations and ratios was mainly ascribed to the seagrass meadow
51 decline through direct (less nutrient consumption) and indirect (increase in phytoplankton
52 biomass) processes. Changes in temperature and wind direction may also influenced the
53 nutrients concentrations through processes of remineralisation and flushing time,
54 respectively. This study illustrates (1) the top-down control of seagrass on the nutrients
55 concentrations and stoichiometry, and (2) the competition between primary producers
56 (seagrass vs phytoplankton) for their nutrients resource.

57

58 1. Introduction

59 Primary production in coastal ecosystems is mainly controlled by the input and the recycling
60 of nutrients — mainly nitrogen (N), phosphorus (P) and silicon (Si) — and their availability
61 (Bouwman et al., 2013; Nixon et al., 1986). Hence, nutrients availability can indirectly affect
62 all trophic levels through bottom-up effects, and therefore influence ecosystems structure
63 and functioning (Borum and Sand-Jensen, 1996; Bouwman et al., 2013; Nielsen and
64 Richarson, 1996). Nutrients mostly enter coastal ecosystems through river discharge
65 (Seitzinger et al., 2002). While N and P are mostly by-products of human activities (such as
66 agrarian activities that induce the use and release of fertilizers), or urban and industry
67 settlement along the waterways (that release waste-waters; (Galloway et al., 2004, Metson
68 et al., 2017)), Si mostly comes from natural weathering (Tréguer et al 1995).

69 Anthropogenic activities disturb the three N, P and Si coastal biogeochemical cycles
70 (Lerman et al., 2004) principally due to modifications on the watershed. Intensive
71 agriculture (including fertilizer use and irrigation) and land artificialisation (including urban
72 expansion and power dam creation) are responsible for changes in N, P and Si
73 concentrations in the rivers (Ragueneau et al., 2006; Rosier and Ritchie, 2013) and
74 consequently in the coastal ecosystems. During the past century, the export of nutrients
75 from the continent to the coastal ecosystems has almost doubled (Beusen et al., 2016) due
76 to the human activities (Paerl 2009). During the second half of the twentieth century, the
77 world population increased by 2.5 folds (United Nation, Department of Economic and Social
78 Affairs, Population Division, 2019) and the food and fertilizers productions increased
79 respectively by 3 and more than 4 folds (Roser and Ritchie, 2013). Anthropogenic activities
80 also affect the atmospheric nutrient input to marine ecosystems: the di-nitrogen fixation

81 along with the dissolved N-deposition from the atmosphere have greatly increased, mainly
82 due to fossil fuel combustion (Bouwman et al., 2013; Seitzinger et al., 2002; Xenopoulos et
83 al., 2017). Such alteration of the biogeochemical cycles (nutrient concentrations and ratios)
84 can increase eutrophication episode rates and magnitudes (Ménèsguen and Piriou, 1995;
85 Sinha et al., 2017) that affect the whole ecosystem, from phytoplankton assemblages,
86 sediment and benthic communities, to top trophic levels (Cloern, 2001).

87 Following the growing concern and knowledge on eutrophication, human societies have
88 implemented management policies to regulate the nutrients export to the coastal
89 ecosystems in the recent decades (i.e. the 1972 US Clean Water Act (33 U.S.C.), the 1991
90 EU Nitrates Directive (Directive 91/676/EC)). Recent studies in various developed countries
91 pointed out decreasing N and P concentrations in the coastal ecosystems during recent
92 decades, leading to various and numerous impacts. In the Chesapeake bay, the nitrate +
93 nitrite inputs increased by 90% between 1945 and 1980 and then decreased by 5.3%
94 between 1981 and 2012 due to nutrient-management strategies launched in the 1980s
95 (Harding et al., 2016). Due to these N loads reduction, more areas in Chesapeake bay were
96 N-limited or not subjected to apparent nutrient limitation (Zhang et al., 2021). In Moreton
97 bay (Australia), the implementation of a sewage treatment plant helped to reduce the
98 dissolved nitrogen export leading to a decrease of the N:P ratio as well as of the
99 chlorophyll-a concentrations (Saeck et al., 2013). The nutrients exported to the San
100 Francisco bay also decreased but it led to an increase of the phytoplankton biomass
101 through cascade effects following the decrease of their predators' population (Cloern et al.,
102 2007). In the Baltic sea, the dissolved Si concentration decreased at the end of the
103 twentieth century and it had been attributed to a decrease in the river Si export (Conley et
104 al., 2002), following the implementation of dams in the watershed (Papush and Danielsson,
105 2006). Although clear evidences of recovery from eutrophication occurred following large

106 reduction in nutrients concentrations like in Boston Harbor (Taylor et al., 2020), a lack of
107 response could occur when nutrients concentrations reductions were weaker (Duarte et al.,
108 2008). This highlighted that even though extra human-induced nutrients loads played a key
109 role in coastal ecosystems eutrophication, it was not the only parameter to take into
110 account to reduce eutrophication because the response of ecosystems are non-linear and
111 complex (Cloern et al., 2010), and because ecosystems could change from a state
112 equilibrium to another (Scheffer & Carpenter, 2003, Scheffer et al., 2009) towards the re-
113 oligotrophication process.

114 Coastal ecosystems and their intrinsic functioning are not only under the direct
115 anthropogenic influence but also under climatic influence. The climatic influence is
116 expressed through a large set of drivers such as precipitations, temperature and wind
117 circulation (Bouwman et al., 2013). For instance, the atmospheric deposition, enhanced by
118 the precipitations, can induce phytoplankton blooms in some ecosystems (Durrieu de
119 Madron et al., 2011). Solar radiation and the associated temperature increase enhance
120 water stratification, which reduces the amount of vertical input from deeper waters (Doney
121 2006). Also, wind circulation — and tides — can modify hydro- and sediment dynamics
122 (Christiansen et al., 2006) and thus favour benthic nutrient input to the water column in
123 shallow ecosystems.

124 Within this context of long-term changes in nutrients inputs under anthropogenic and
125 natural drivers, we investigated (i) the bi-decadal (1999 – 2018) inter-annual and seasonal
126 changes in nutrients concentration and ratios, (ii) their spatial variability, and (iii) their
127 drivers at local and large scales in a semi-enclosed and poorly-anthropized ecosystem that
128 also experienced primary producers long-term changes: the Arcachon bay, France.

129 **2. Material and Methods**

130 **2.1 Study site**

131 The Arcachon bay is a 180 km² semi-enclosed lagoon located on the South-western coast
132 of France (Figure 1). It faces a semi-diurnal meso- to macro-tidal regime (0.8 to 4.6 m) and
133 has an average depth of 4.6 m and a maximum depth of 20 m in the main channels. The
134 channels run through large intertidal mudflats that account for two third of the total surface
135 area of the bay. Freshwater mainly comes from the Leyre River (75%) with an average flow
136 of 1.3×10^6 m³ per day, from two man-regulated canals (Porge canal and Landes canal)
137 and from several small streams. Freshwater inputs are low compared to ocean water tidal
138 exchange (ca. 400×10^6 m³ in average). In this bay, three main water masses were defined
139 (Bouchet 1968, Robert et al., 1987): (i) the external neritic waters (ENW), directly influenced
140 by the oceanic waters (the highest salinity and the lowest annual salinity and temperature
141 amplitudes), (ii) the intermediate neritic waters (ItNW) and (iii) the inner neritic waters
142 (InNW), particularly influenced by the continental inputs (the lowest salinity and the highest
143 annual salinity and temperature amplitudes).

144 The watershed of the Arcachon bay has an area of 3500 km². It is mainly covered by forests
145 (ca 80%) and agricultural lands (ca 10%). The urban areas (5%) are mainly located along
146 the bay coastline. The urban effluents are derived since the 1970s and released after
147 treatment in the Atlantic waters outside of the bay (Figure 1). This ecosystem can therefore
148 be considered as poorly anthropized.

149 The intertidal flats of the bay are colonized by dwarfgrass (*Z. noltei*), while eelgrass (*Z.*
150 *marina*) occupies the shallow subtidal sector around the channel edges. The area colonized

151 by these two species drastically declined during the past decades (Plus et al., 2010).
152 Between 1989 and 2007, the total area of *Z. noltei* meadows has decreased by 33% (from
153 68.5 km² to 45.7 km²) while the area of *Z. marina* meadows has decreased by 74% (from
154 3.7 km² to 1.0 km²). Between the 1980s and 1990s, macroalgae proliferations were
155 reported in the bay, *Enteromorpha clathrata* since 1985 and *Monostroma obscurum* since
156 1989 (Auby et al., 1994; Ménesguen et al., 1997), but these blooms are no longer observed
157 at present. The bay is also an important mariculture site, especially for the oyster
158 *Crassostrea gigas* farming and production of spats (Buestel et al., 2009), and is the main
159 site for the production of Manilla clam *Ruditapes philippinarum* in France (Caill-Milly et al.,
160 2008).

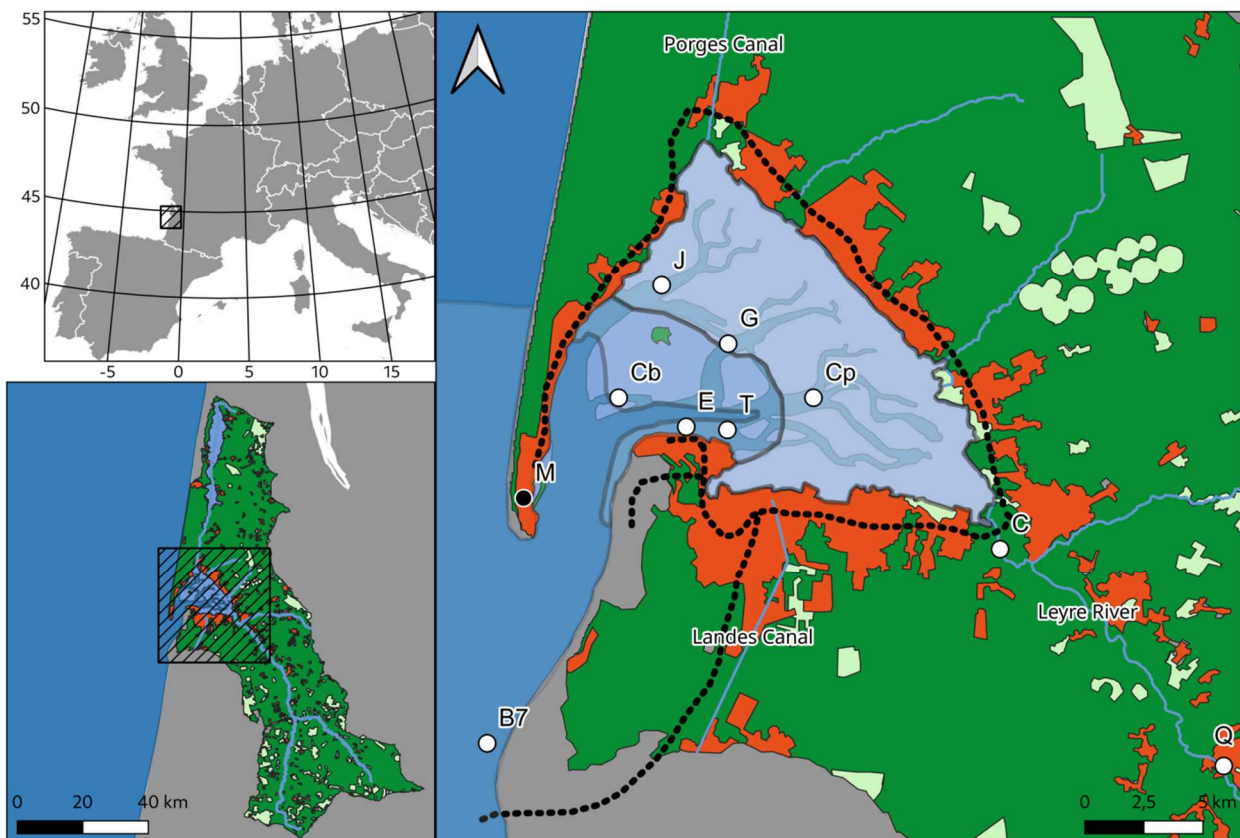


Figure 1 : The Arcachon bay with the location of the sampling sites and water masses. Cp: Comprian; T: Tès; G: Girouasse; E: Eyrac; J: Jacquets; Cb: Courbey and B7: Bouée 7 are the seven coastal sampling sites in the bay, C: site recording the nutrients concentrations in the Leyre river (Lamothe); Q: site recording

the Leyre river discharge (Salles , 2 site on the Leyre river), M: meteorological site (Cap Ferret).

The plain blue lines are the freshwater inputs and the black dotted line represents the main urban effluents tubes. The background colours represent the land use: red for urban lands; light green for agricultural lands; dark green for forestial lands; gray for land outside the Arcachon bay watershed, light blue for intertidal water and dark blue for subtidal waters (Corine Land Cover, 2018). The shades delimit the external (western side), intermediate (in the middle) and internal (eastern side) neritic waters (adapted from Bouchet (1968)).

161

162 **2.2 Data**

163 The present study is based on data sets stored in different databases (Table 1). These data
164 sets gather nutrients concentrations in the Arcachon bay (core parameters of the study) as
165 well as parameters indicators of environmental drivers used as explanatory variables.
166 These latter parameters were selected as proxies of processes potentially linking drivers
167 and nutrients. For instance, salinity can be considered as a proxy of freshwater inputs,
168 riverine nutrients concentrations can be considered as a proxy of nutrient river load,
169 meteorological parameters relate to the climatic influence.

170 All the data were analysed from March 1999 to December 2018. Data providers are
171 reported in Table 1.

172

173 **2.2.1 Arcachon bay data**

174 In the bay, two monitoring programs are running: ARCHYD, a local survey that samples
175 seven sites weekly, alternately at high and low tide, some from 1989 and others from 2007;
176 and SOMLIT, a national network that samples, in this bay, three stations bi-monthly at high
177 tide some from 1997 and others from 2005. For the present study six ARCHYD sites
178 (Bouée 7 in the ENW, Courbey and Tès in the ItNW, and Comprian, Girouasse and
179 Jacquets in the InNW) and one SOMLIT site (Eyrac in the ItNW) were selected based on

180 their sampling duration and monitored parameters. Bouée 7, Comprian and Jacquets are
181 also sites monitored within the REPHY which is another national network. These programs
182 participated to inter-laboratory exercises, both at the local and national scales (Belin et al,
183 2021; Breton et al., *in prep*).

184 In the following, low tide and high tide (LT and HT respectively) samplings are differentiated
185 for each site (e.g. Tès LT versus Tès HT). Sites refer to geographic position and stations
186 refer to the combination of a site and a tidal moment.

187 The nutrients used in this study are: nitrate + nitrite (NO_x), ammonium (NH_4^+), dissolved
188 orthophosphates (PO_4^{3-}) and silicic acid ($\text{Si}(\text{OH})_4$). NO_x and NH_4^+ were summed before
189 calculating the Si:N and N:P ratios. Water temperature, salinity, suspended particulate
190 matter (SPM) and chlorophyll-*a* were selected as proxies of potential drivers. In the
191 following, they are referred to as ‘biophysical parameters’. For more information regarding
192 these programs, see Cocquempot et al., (2019), Goberville et al., (2010) and Liénart et al.,
193 (2017, 2018) for SOMLIT, and Ifremer (2017) for ARCHYD.

194

195 **2.2.2 Continental data**

196 Three continental variables were collected: two nutrients (NO_x and NH_4^+) and the river
197 discharge (Q). The nutrients were monitored at Lamothe and the discharge at Salles
198 (Figure 1), upstream the dynamic influence of the tide. These data sets were provided by
199 EauFrance and the Adour-Garonne water agency.

200

201 **2.2.3 Climate data**

202 **2.2.3.1 Local-scale climate**

203 Seven meteorological variables were used: four atmospheric circulation variables (the
204 atmospheric pressure at sea-level, the wind intensity and its meridional and zonal
205 components), along with the air temperature, the short wave irradiation and the monthly
206 accumulated mean precipitation. The meteorological variables were obtained from the
207 MeteoFrance forecast weather station located at Cap Ferret. The short wave irradiation was
208 a reconstructed variable provided by MERRA-2 (see Gelaro et al., 2017).

209 Extra attention is called on the directional components on the wind. As these variables are
210 made from the scalar product between the wind intensity and its direction, they can
211 potentially take values between minus and plus infinity. Winds coming from the North (wind
212 direction strictly over 270° and strictly under 90° based on a wind rose) and wind coming
213 from the South are depicted by negative and positive meridional wind speeds respectively.
214 Winds coming from the East (wind direction strictly over 0° and strictly under 180°) and
215 winds coming from the West are depicted by negative and by positive zonal wind speeds
216 respectively. Winds coming from the exact North/South or East/West have null meridional or
217 zonal speeds respectively. Therefore, increasing negative meridional or zonal speeds depict
218 increasing winds from the North or the East, respectively. Meridional or zonal speeds close
219 to 0 mean null wind intensity along their respective axis.

220 **2.2.3.2 Large-scale climate**

221 Five hydro-climatic indices were used: the Atlantic Multidecadal Oscillation (AMO), the
222 Northern Hemisphere Temperature anomalies (NHT), the East Atlantic Pattern (EAP), the
223 Northern Atlantic Oscillation (NAO) and the Arctic Oscillation (AO). The AMO (Enfield et al.,

224 2001) represents the changes in the north Atlantic sea surface temperature after removing
225 the human impact whereas the NHT anomalies is an index based on the 1901-2000 north
226 Atlantic temperature average. The NAO (Hurrell 1995; Hurrell & Deser 2009) and the EAP
227 (Barnston & Livezey 1987) are the two most predominant mode of low-frequency variability
228 over the north Atlantic. While the NAO tracks the movements of the Azores high, the EAP
229 values consist of a north-south dipole of pressure anomalies centred on the north Atlantic,
230 from east to west. Finally, the AO is based on atmospheric pressures and is related to the
231 Arctic climate and its southern incursions. The data was provided by the US National
232 Oceanic and Atmospheric Administration (NOAA) National Center for Atmospheric
233 Research (NCAR), Climate Prediction Center (CPC) and National Centers for
234 Environmental Information (NCEI).

235

237 *Table 1 : Variables, providers and associated website for the Arcachon bay, the main river, meteorological data and large scale hydro-climatic indices from*
 238 *March 1999 to December 2018.*

Type	Variables	Provider	Website
Coastal ecosystem	NO _x , NH ₄ ⁺ , PO ₄ ³⁻ , Si(OH) ₄ , wT, S, SPM, CHLA	SOMLIT	www.somlit.fr
		ARCHYD	https://wwz.ifremer.fr/surval https://doi.org/10.17882/47248
Leyre river	NO _x , NH ₄ ⁺ , SPM Q	Eau france	http://www.naiades.eaufrance.fr/ http://www.hydro.eaufrance.fr/
Meteorological data	aT, lwind, Vwind, Uwind, MP, P	Meteo-France	https://donneespubliques.meteofrance.fr/?fond=contenu&id_contenu=37
	W	MERRA-2	http://www.soda-pro.com/fr/web-services/meteo-data/merra
Large-scale hydro-climatic indices	AMO		https://www.esrl.noaa.gov/psd/data/timeseries/AMO/
	AO		https://www.cpc.ncep.noaa.gov/products/precip/CWlink/daily_ao_index/monthly.ao.index.b50.current.ascii
	EAP	NOAA, NCAR, CPC, NCEI	https://www.cpc.ncep.noaa.gov/data/teledoc/ea.shtml
	NAO		https://climatedataguide.ucar.edu/climate-data/hurrell-north-atlantic-oscillation-nao-index-station-based
	NHT		https://www.ncdc.noaa.gov/monitoring-references/faq/anomalies.php#anomalies

239 **2.3 Statistical analyses**

240 In order to standardise all the time series, the data was aggregated to the month by
241 applying a median if more than one observation were available for each month. In this
242 study, all the time series have 238 values (238 months from March 1999 to December
243 2018) based on the available data and the maximum lag in the raw data.

244 Nutrients, SPM and chlorophyll-a concentrations as well as river discharge data were log-
245 transformed prior to any other statistical treatment.

246

247 **2.3.1 Time series decomposition**

248 Each time series, except the hydro-climatic indices, was decomposed using dynamic linear
249 models (DLMs; West and Harrison, 1997). The DLM approach had already been used
250 successfully with environmental data series (Hernandez-Farinas et al 2014, Ratmaya et al.
251 2019). They can be viewed as a dynamic version of linear models: their parameters are
252 allowed to vary with time. The model that has been used here decompose each time series
253 into an inter-annual component and a seasonal component. This model is based on a
254 second-order polynomial that, when appropriate, can produce a quadratic inter-annual
255 component. The time varying seasonal component is based on a trigonometric function with
256 two harmonics that allow the expression of bi-modal patterns (e.g. spring and autumn
257 blooms). As outliers may have strong influence on models, a procedure has been set up to
258 identify and treat them. Data were considered as outliers when their standardized residuals
259 were outside the interval defined by the whiskers of a box-and-whiskers plot applied to a
260 standardized gaussian distribution: in other words, outliers were the 0.35% higher values
261 and the 0.35% lower values. Different models were run following an iterative process where

262 identified outliers were given a proper observational variance so that they had less weight.
263 This step was repeated until no more outliers were detected. DLMS were applied with the
264 dlm package (Petris, 2010) using the R software (R Development Core Team, 2021).
265 Residuals of the models are used to assess their validity. The normality of the residuals
266 was checked using a Q-Q plot and tested with the Kolmogorov-Smirnoff test (Kolmogorov,
267 1933); the residuals independence was checked with plots of estimated auto-correlation
268 function and tested with the Stoffer-Toloi modified test (Stoffer and Toloi 1992); and finally,
269 the homoscedasticity was tested with the Goldfeld-Quandt test (Goldfeld and Quandt, 1965).
270 The models used in the study were those answering to the most of these conditions and
271 with the smaller Akaike Information Criterion (AIC).

272

273 **2.3.2 Bi-decadal trends**

274 A modified Mann-Kendall test (Yue and Wang, 2004) was applied on the DLMS inter-annual
275 components to assess the significance of the bi-decadal changes (i.e. presence of a
276 positive or negative monotonic linear long-term trend). When a significant trend was
277 detected, the Sen's line (Helsel and Hirsh, 2002) was used to calculate the amplitude of
278 change that occurred between 1999 and 2018. The modified Mann-Kendall was chosen
279 upon the regular Mann-Kendall test in order to remove the serial correlation effect on the
280 test on hydrobiological time series that have autocorrelation.

281

282 **2.3.3 Nutrient ratios**

283 Nutrient ratios (Si:N, N:P, Si:P) were calculated from the nutrients monthly medians. The
284 value for each month was then compared to the extended Redfield ratio $N_{16}:P_1:Si_{16}$

285 (Harrison et al., 1977) in order to calculate the most potentially limiting nutrient. Six
286 combinations were thus possible (from the most to the lesser probably limiting nutrient:
287 P:N:Si, P:Si:N, N:P:Si, N:Si:P, Si:N:P, Si:P:N). One should keep in mind that deviation from
288 the Redfield ratios gives an information on the potential limitation of phytoplankton growth
289 by nutrients but is not a measure of 'real' limitation. The latter also depends on the nutrient
290 concentrations and phytoplankton intrinsic physiology (i.e. Km constants). Thus, none, one
291 or even all the nutrients could (co-)limit phytoplankton growth depending on the difference
292 between their concentrations and the Km constants.

293

294 **2.3.4 Potential abiotic drivers**

295 The potential abiotic drivers influence was assessed using Partial Least Square Path
296 Modeling (PLS-PM). PLS-PM models were applied using the plsmpm package (Sanchez,
297 2013) in the R software (R Development Core Team, 2021). PLS-PM enable to study the
298 links between blocks of variables. The blocks are defined *a priori*, and the links are
299 estimated by ordinary least squares in multiple linear regressions (Sanchez, 2013). PLS-
300 PM are made of two sets of linear equations. The first set define the inner model
301 (measurement model) that determines the links between the latent variables (LV;
302 unobservable variables). The second set define the outer model (structural model) that
303 identifies the links between one LV and its manifest variables (MV; observable variables).
304 The PLS-PM framework consists of building successive models that are assessed, before
305 reaching to the final model. The temporal auto-correlation was taken into account using the
306 Chatfield (1996) modified Box-Jenkins auto-correlation function (Box & Jenkins 1976)
307 coupled with the Chelton formula (Chelton, 1984) to adjust the degrees of freedom in the
308 correlation between the MVs. An auto-correlation correction (AR1) was applied to the linear

309 models of the outer model. Path coefficients are used to estimate the relative influence of a
310 block onto another. Path coefficients are close to multiple linear regression coefficients
311 meaning that they depict standard deviations changes around the mean.

312 A few requirements are needed before reaching the final PLS-PM model. First, the
313 unidimensionality of the loadings is required, (i.e. all the correlations between MVs need to
314 be of the same sign). Therefore when a loading is negative, the opposite of the data is
315 taken. Secondly, it is recommended to keep only MVs with loadings higher than 0.7
316 (Sanchez, 2013). An iterative process was applied here so that after the removal of the
317 weakest MV, a new model was made using the remaining MVs, until all the loadings were
318 over 0.7. This was preferred rather than removing all the loadings that did not meet this
319 requirement, in order to stay as close as possible to the iterative properties of the PLS-PM
320 algorithm.

321 In this study, six blocks of variables were used: the Large scale Climate (AMO, AO, EAP,
322 NAO, NHT), the Local Climate (lwind, Uwind, Vwind, P, MP, W, aT), the River (Q, NO_x,
323 NH₄⁺), the Ecosystem characteristics (S, SPM, wT) and the Nutrients separated into two
324 blocks (NO_x, NH₄⁺, Si(OH)₄ in the first and PO₄³⁻ in the second). A total of 14 links were
325 considered. The Large scale climate could influence the five other blocks, the Local climate
326 all the other blocks but the large scale climate, the River nutrients could influence the
327 Ecosystem characteristics and the two Nutrients blocks and finally the Ecosystem
328 characteristics could influence the two Nutrients blocks. Only the significant relationships
329 were considered. As the goal of these models was to point out the drivers influencing the
330 nutrients, if the loading of a nutrient was lower than 0.7 a new block was created with the
331 concerned nutrient instead of removing it.

332 The goodness of fit of the models ranged between 0.49 and 0.74.

333 **3. Results**

334 **3.1. Nutrient bi-decadal changes in the bay waters**

335 **3.1.1 Overview of the spatial and temporal nutrients changes**

336 In the Arcachon bay, the main freshwater inputs come from the Leyre river at the
337 southeastern end of the bay. Hence, a salinity gradient exists between the Leyre mouth
338 (mean over the studied period: 29.0 ± 4.4 at Comprian) and the channel to the ocean
339 (mean over the studied period: 34.4 ± 0.8 at Bouée 7), at the southwestern side of the bay.
340 Gradients of nutrients are associated to this salinity gradient. Winter concentration of NO_x
341 averaged $42 \mu\text{M}$ at Comprian LT and $4.8 \mu\text{M}$ at Bouée 7 HT, with maximum values up to
342 136 and $13.4 \mu\text{M}$ respectively. Winter concentration of $\text{Si}(\text{OH})_4$ averaged $49 \mu\text{M}$ at
343 Comprian LT and $4.3 \mu\text{M}$ at Bouée 7 HT, with maximum values up to 105 and $13.0 \mu\text{M}$
344 respectively. The seasonality of these nutrients is large with summer values often lowering
345 to $0.1 \mu\text{M}$. The seasonal variations are larger in the InNW than in the ENW by a factor of ca
346 10 . Overall, PO_4^{3-} ranges between 0.02 and $0.96 \mu\text{M}$, with higher values usually
347 encountered in winter and autumn in the InNW, and NH_4^+ between ca 0.05 and $17.0 \mu\text{M}$,
348 with higher values usually encountered in winter and autumn in the InNW. In the whole data
349 set considered in the present study, mean values of NO_x , NH_4^+ , PO_4^{3-} and $\text{Si}(\text{OH})_4$ are 7.8 ,
350 2.3 , 0.11 and $13.7 \mu\text{M}$ respectively.

351

352 **3.1.2 Bi-decadal inter-annual variability**

353 In the following, and for convenience, the results are reported for only two contrasted
354 stations: Comprian LT in the InNW (the most influenced by the Leyre river) and Courbey HT
355 in the ItNW (the inner station the most influenced by oceanic inputs). The other figures are
356 available in Supplementary Material. Table 2 presents the changes in nutrients
357 concentration at all the stations when a trend was detected using a modified Mann-Kendall
358 test (p -value < 0.05 ; Yue and Wang, 2004).

359 Nutrients concentrations in the Arcachon bay evolved similarly regardless of the different
360 water masses (Figure 2; Supplementary Material A). The NO_x inter-annual components
361 significantly increased (according to the modified Mann-Kendall test (Yue and Wang, 2004))
362 at all the stations. The NO_x concentrations were multiplied by 3 to 4 folds in the InNW — the
363 strongest absolute change was recorded at Comprian LT — and by 1,5 fold in the ENW
364 (Table 2). The NH_4^+ inter-annual components significantly increased at 6 out of 13 stations
365 (Table 2), either in the ItNW or in the InNW and at high or low tide. The strongest changes
366 occurred in the InNW, where the nutrients were the most concentrated. The strongest NH_4^+
367 concentration change occurred in the InNW at Jacquets (Supplementary Material A) that is
368 under the direct influence of the Porge canal — the second most important tributary to the
369 bay. The PO_4^{3-} inter-annual components significantly decreased at all the stations but
370 Jacquets LT (no trend). The strongest PO_4^{3-} concentrations decrease occurred in the ENW
371 and the weakest in the InNW. The $\text{Si}(\text{OH})_4$ inter-annual components showed similar
372 patterns to NO_x , with a significant increase at all stations of the ItNW and InNW (with the
373 exception of Tès HT) however not in the ENW. The $\text{Si}(\text{OH})_4$ concentrations were multiplied
374 by 3 to 4 folds in the InNW (strongest absolute change in Comprian LT), and by 1.5 in the
375 ItNW.

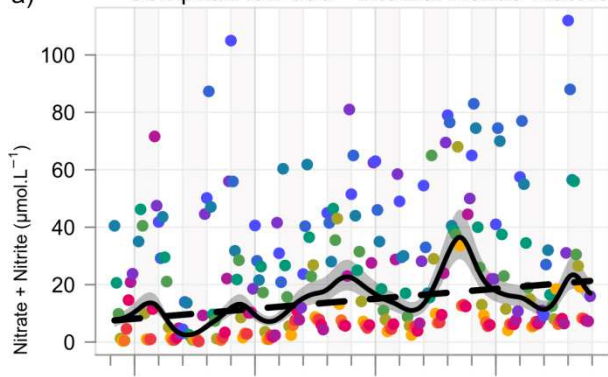
376 Table 2: Bi-decadal (1999 – 2018) trend changes of all the nutrients at all sites based on the modified Mann-Kendall test (Yue and Wang, 2004). Values are the
 377 relative (%) and absolute (Δ in μM) change when it was significant (p -value < 0.05). The stations are displayed following a decreasing continental influence, from low
 378 tide to high tide.

379

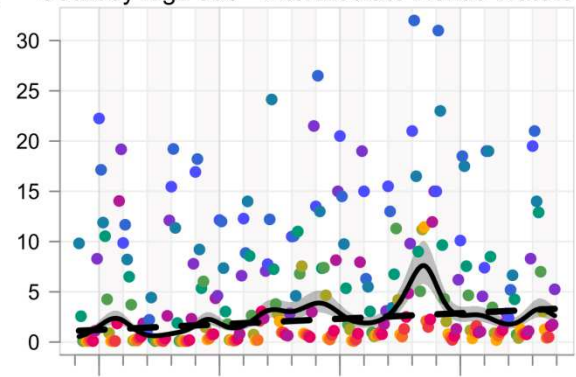
		Inner Neritic Waters						Intermediate Neritic Waters					External Neritic Waters	
		Comprian LT	Comprian HT	Girouasse LT	Girouasse HT	Jacquets LT	Jacquets HT	Eyrac HT	Tès LT	Tès HT	Courbey LT	Courbey HT	Bouée 7 LT	Bouée 7 HT
NO _x (μM)	%	+182	+337	+312	+350	+279	+240	+412	+354	+186	+142	+194	+53	+16
	Δ	+13.7	+4.9	+4.3	+4.2	+2.6	+2.5	+4.7	+8.1	+2.3	+1.6	+2.2	+0.5	+0.1
NH ₄ ⁺ (μM)	%	ns	+88	ns	ns	+265	+120	+2	ns	+32	+85	ns	ns	
	Δ	ns	+1.4	ns	ns	+2.5	+1	+0.02	ns	+0.4	+0.9	ns	ns	
PO ₄ ³⁻ (μM)	%	-16	-38	-21	-36	ns	-34	-59	-27	-57	-36	-41	-51	-54
	Δ	-0.03	-0.05	-0.02	-0.05	ns	-0.03	-0.10	-0.04	-0.07	-0.04	-0.05	-0.05	-0.05
Si(OH) ₄ (μM)	%	+94	+65	+49	+49	+100	+64	+70	+63	ns	+55	+32	ns	ns
	Δ	+21.6	+6.1	+6.2	+5.0	+11.7	+4.7	+4.1	+9.40	ns	+4.3	+2.4	ns	ns

380

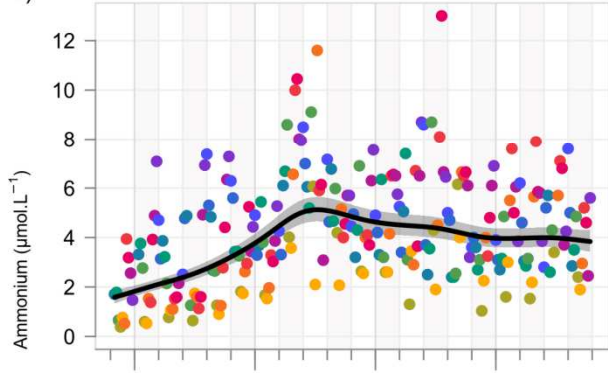
a) Comprian low tide - Internal Neritic Waters



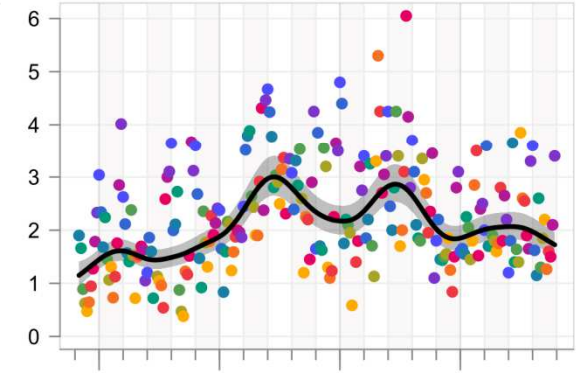
b) Courbey high tide - Intermediate Neritic Waters



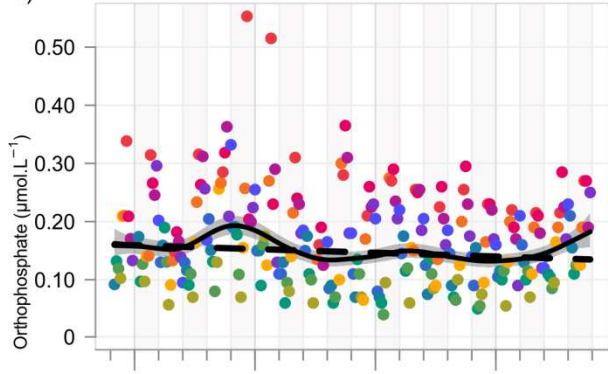
c) Comprian low tide - Internal Neritic Waters



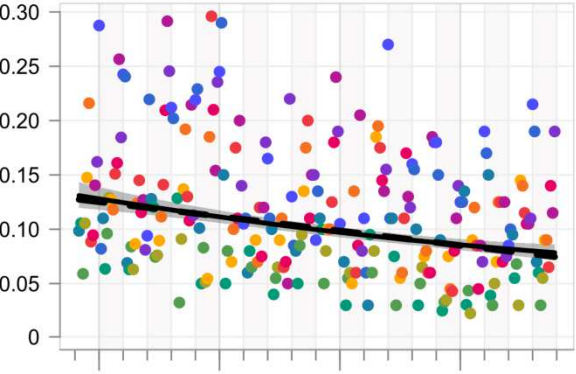
d) Courbey high tide - Intermediate Neritic Waters



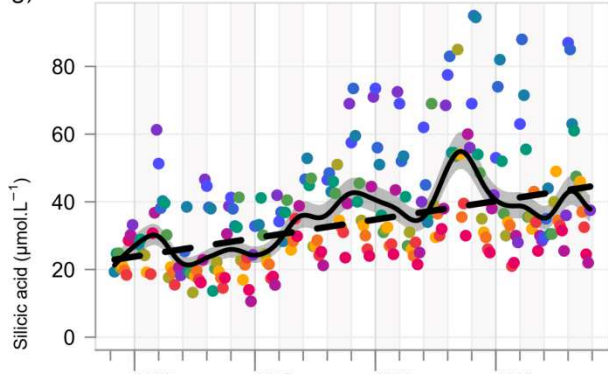
e) Comprian low tide - Internal Neritic Waters



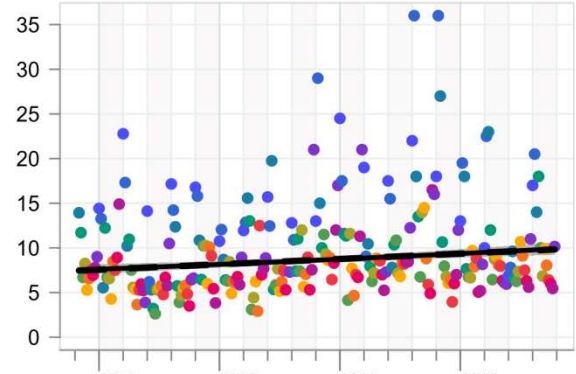
f) Courbey high tide - Intermediate Neritic Waters



g) Comprian low tide - Internal Neritic Waters



h) Courbey high tide - Intermediate Neritic Waters



Years

Years

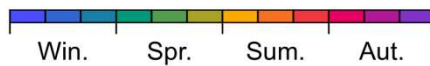


Figure 2: Bi-decadal inter-annual component of nitrate + nitrite (a,b), ammonium (c,d), orthophosphate (e,f) and silicic acid (g,h) at two contrasted stations: Comprian low tide (a, c, e, g) and Courbey high tide (b, d, f, h), respectively representative of the inner and intermediate neritic waters in the Arcachon bay. In each panel, the plain black line is the DLM bi-decadal inter-annual component, the gray shadow is its confidence interval at 90%, the dots are the observations for each month coloured in function of the season. The bi-decadal change was estimated with a modified Mann-Kendall test (Yue and Wang, 2004). When the test was significant, the Sen's line was drawn in dashed black.

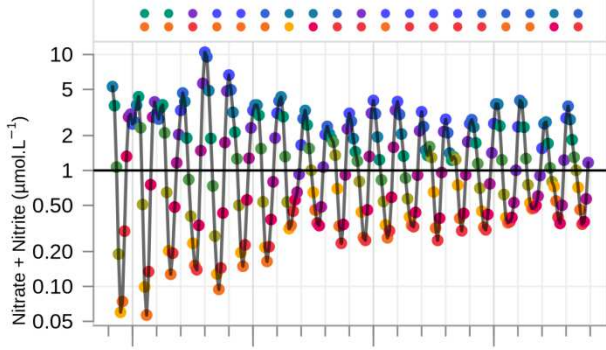
381 3.1.3 Bi-decadal seasonality

382 In addition to the overall concentration increase (NO_x , of NH_4^+ , $\text{Si}(\text{OH})_4$) or decrease (PO_4^{3-})
383 across the bay, seasonal patterns were modified during the 20 studied years (Figure 3,
384 Supplementary Material B).

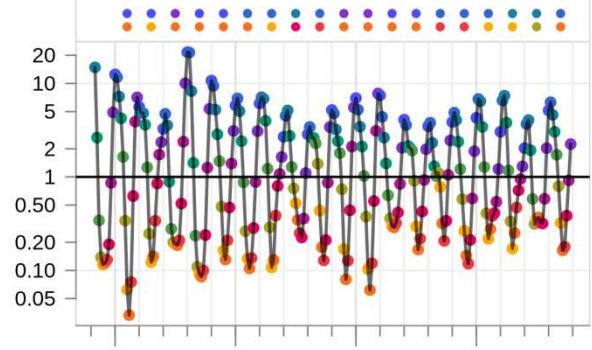
385 The seasonal component amplitude of NO_x decreased at almost all the stations and was
386 related to both an increase of the minimal (ca. summer) values and a decrease of the
387 maximal (ca. winter) values. In the InNW and the ItNW, the occurrence of the seasonal
388 maximum did not change over the time period whereas the occurrence of the seasonal
389 minimum occurred later in summer. It remained stable in the ENW. The seasonal
390 component amplitude of NH_4^+ decreased at most of the stations in relation to the decrease
391 of the maximal values in autumn and winter and to the increase of the minimal values in
392 summer. The occurrence of the seasonal maximum was advanced by a couple of months at
393 most of the stations from winter to autumn, regardless the tide and the water mass (e.g.
394 Figure 3c). The occurrence of the seasonal minimum remained stable at most of the
395 stations, but it was advanced from July to June at Comprian LT (e.g. Figure 3c). The
396 strongest changes occurred in the ItNW and ENW. The seasonal component amplitude of
397 PO_4^{3-} increased at most of the stations except in the InNW where it remained stable (e.g.
398 Figure 3e, f). This increase coincided with an increase of the maximal values in winter and
399 a decrease of the minimal values in summer. The occurrence of the seasonal maximum
400 and minimum were delayed from autumn to winter and from spring to summer, respectively.

401 The seasonal component amplitude of Si(OH)_4 either remained quite stable or increased.
402 The increasing amplitude coincided more with an increase of the maximal values in winter
403 than to a decrease of the minimal value. The occurrence of the seasonal maximum
404 remained stable in winter or was delayed from December to January at some stations and
405 the occurrence of the seasonal minimum was often delayed from spring to autumn (see
406 Supplementary Material B).

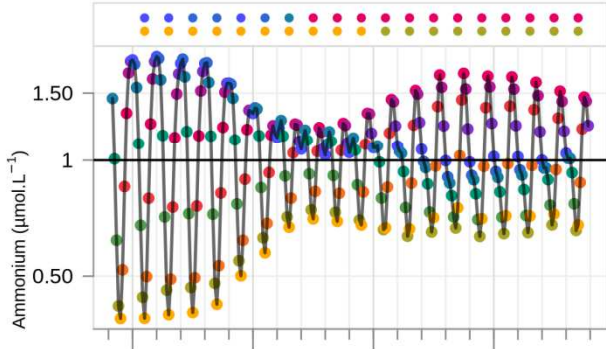
a) Comprian low tide - Internal Neritic Waters



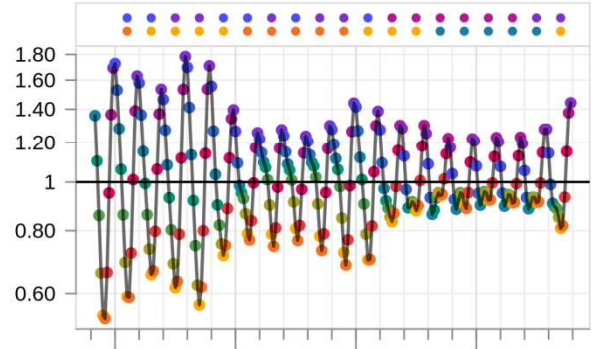
b) Courbey high tide - Intermediate Neritic Waters



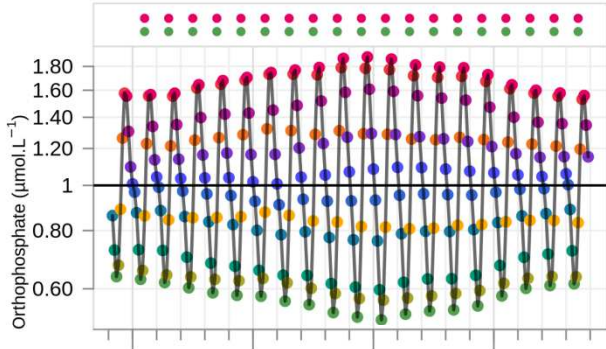
c)



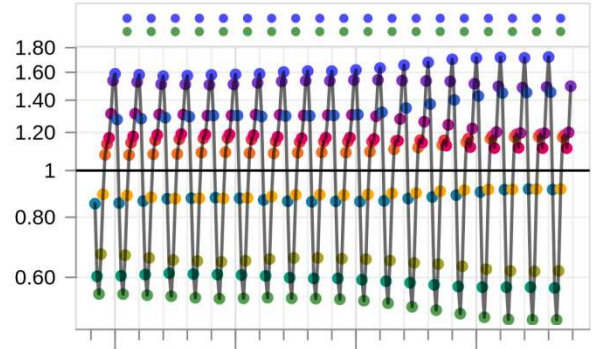
d)



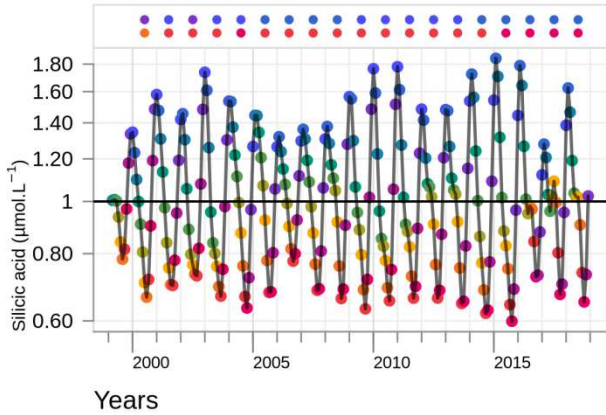
e)



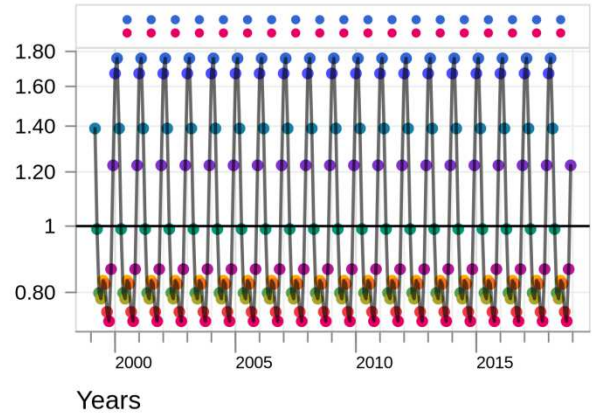
f)



g)



h)



Years

Years

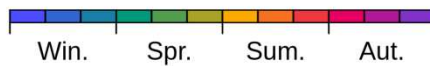


Figure 3: Bi-decadal seasonality of nitrate + nitrite (a,b), ammonium (c,d), orthophosphate (e,f) and silicic acid (g,h) at two contrasted stations: Comprian low tide (a, c, e, g) and Courbey high tide (b, d, f, h), respectively representative of the inner and intermediate neritic waters in the Arcachon bay. The dots are the DLM estimations for each month coloured in function of the season. When seasonal values equal to 1 (horizontal black line), the fitted values were equal to the inter-annual component.

The dots at the top of each graph represent the month of maximum (top) and of minimum (bottom) of seasonality for each complete year.

407

408 **3.1.4 Nutrient ratios**

409 In the Arcachon bay the period of phytoplankton production runs from late February to late
 410 October (Glé et al., 2008). Despite large differences in phytoplankton production among the
 411 three water masses (Glé et al., 2008), the nutrients ratios evolved similarly over the two
 412 decades (Figure 4; Supplementary Material C). At the beginning of the period (ca. 1999-
 413 2003), phytoplankton growth was potentially limited by P in early spring but by N from late
 414 spring to autumn (Figure 4b). However, over the two decades, the potential N limitation
 415 period was shortened from 6-7 month in the early 2000s to 3-4 month in the late 2010s, and
 416 even disappeared at Comprian LT (Figure 4a).

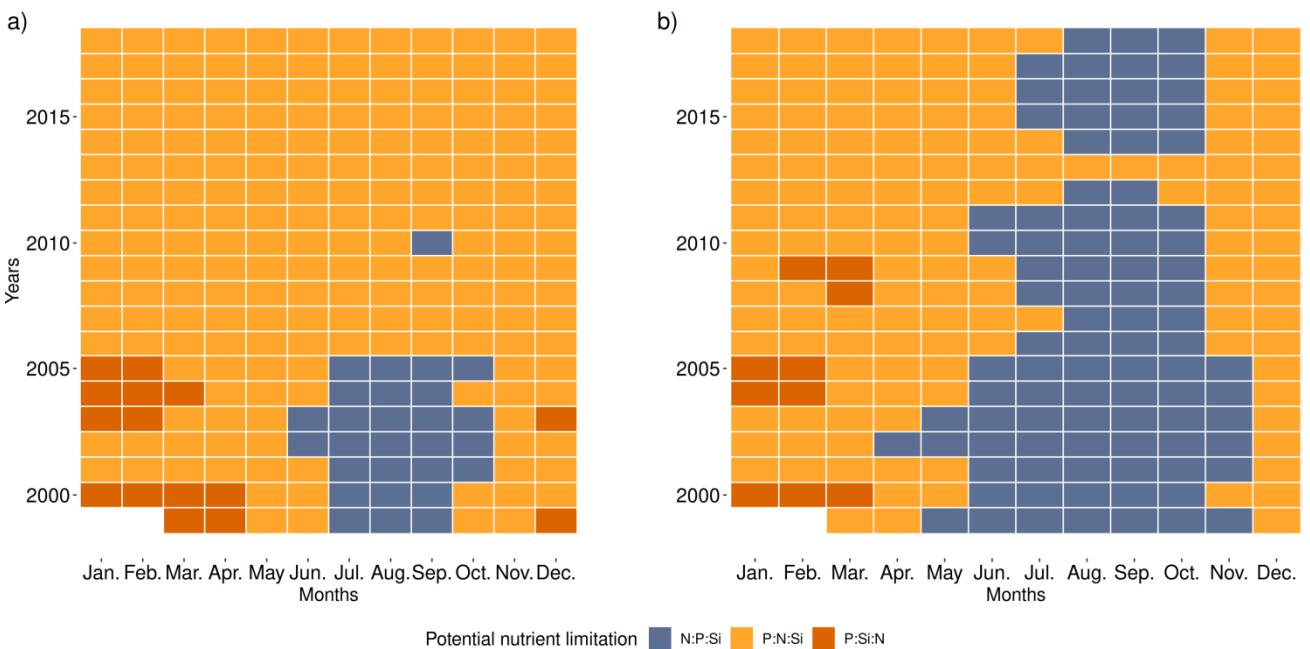


Figure 4: Bi-decadal changes in the potential nutrient-limitation based on the extended Redfield ratio $N_{16}:P_1:Si_{16}$ (Harrison et al., 1977) at two contrasted stations: Comprian low tide (a) and Courbey high tide (b), respectively representative of the inner and intermediate neritic waters in the Arcachon bay. The order of the elements within the ratios indicate the strength of the potential limitation (for instance P:N:Si indicates that N is potentially less limiting than P but more than Si). Note that all the possible combinations were investigated (see section 2.3.3) but that only three were detected.

417

418 **3.2 Bi-decadal changes of possible drivers**

419 **3.2.1. Biophysical parameters of the bay waters**

420 Changes in biophysical parameters were observed concomitantly to changes in nutrients
421 concentrations and ratios (Table 3, Figure 5 and 6, Supplementary Material A and B).

422 The water temperature inter-annual components in the Arcachon bay significantly increased
423 at 7 over 13 stations. The increase was more pronounced in the inner and southernmost
424 part of the bay (e.g. at Comprian and Eyrac HT with an increase of more than 0.4 °C over
425 the two decades; Figure 5a, Table 3). The salinity inter-annual components significantly
426 increased at 3 sites at high tide and showed a high inter-annual variability at all the stations.
427 The SPM inter-annual components significantly increased at low tide at the all the InNW
428 sites and at Tès. The chlorophyll-*a* inter-annual components significantly increased at most
429 of the stations, especially at low tide in the InNW and ItNW (Table 3).

430 The seasonal component amplitude of water temperature remained stable such as the
431 occurrence of the seasonal maximum (July or August) and minimum (January or February).

432 The seasonal component amplitude of salinity remained stable even though there was a
433 high variability in the inter-annual maximal and minimal values. The occurrence of the
434 seasonal maximum remained stable in summer and autumn yet for some years the
435 maximum was in winter or spring. The occurrence of the seasonal minimum remained
436 stable in winter and spring. No clear pattern emerged from the seasonal component

437 amplitude of SPM: it increased (e.g. Courbey HT, Bouée 7 LT), remained stable (e.g.
438 Girouasse LT, Bouée 7 HT) or decreased (e.g. Comprian LT). The seasonal maximum
439 occurred in winter and remained stable at most stations but Comprian LT where it was
440 delayed from winter to summer and Comprian HT where it remained stable in spring. The
441 chlorophyll-*a* seasonal component amplitude remained stable at a majority of stations. The
442 occurrence of the seasonal maximum remained stable in spring or in summer but at
443 Comprian LT where it was delayed from summer to spring. The occurrence of the seasonal
444 minimum remained stable in autumn or winter.

445 Table 3: Table representing the bi-decadal (1999 – 2018) trend changes of the additional parameters at all stations. Values are the relative (%) and absolute (Δ)
 446 in μM) change when it was significant (p -value < 0.05). The stations are displayed following a decreasing continental influence, from low tide to high tide.

		<i>Inner Neritic Waters</i>						<i>Intermediate Neritic Waters</i>					<i>External Neritic Waters</i>	
		Comprian LT	Comprian HT	Girouasse LT	Girouasse HT	Jacquets LT	Jacquets HT	Eyrac HT	Tès LT	Tès HT	Courbey LT	Courbey HT	Bouée 7 LT	Bouée 7 HT
wT	%	+3	+3	ns	+2	ns	ns	+4	ns	+2	ns	ns	+3	+1
(°C)	Δ	+0.52	+0.44	ns	+0.29	ns	ns	+0.56	ns	+0.30	ns	ns	+0.37	+0.10
Sali (psu)	%	ns	ns	ns	+3	ns	ns	ns	ns	+3	ns	+4	ns	ns
	Δ	ns	ns	ns	+0.98	ns	ns	ns	ns	+1.04	ns	+1.17	ns	ns
SPM ($\text{mg}\cdot\text{L}^{-1}$)	%	+72	ns	+164	ns	+107	ns	ns	+62	ns	ns	ns	ns	ns
	Δ	+7.17	ns	+9.90	ns	+5.90	ns	ns	+5.13	ns	ns	ns	ns	ns
CHLA ($\mu\text{g}\cdot\text{L}^{-1}$)	%	+93	ns	+42	ns	+28	ns	+37	+41	+22	ns	+10	+13	+14
	Δ	+2.22	ns	+0.79	ns	+0.62	ns	+0.53	+0.81	+0.36	ns	+0.13	+0.29	+0.22

447

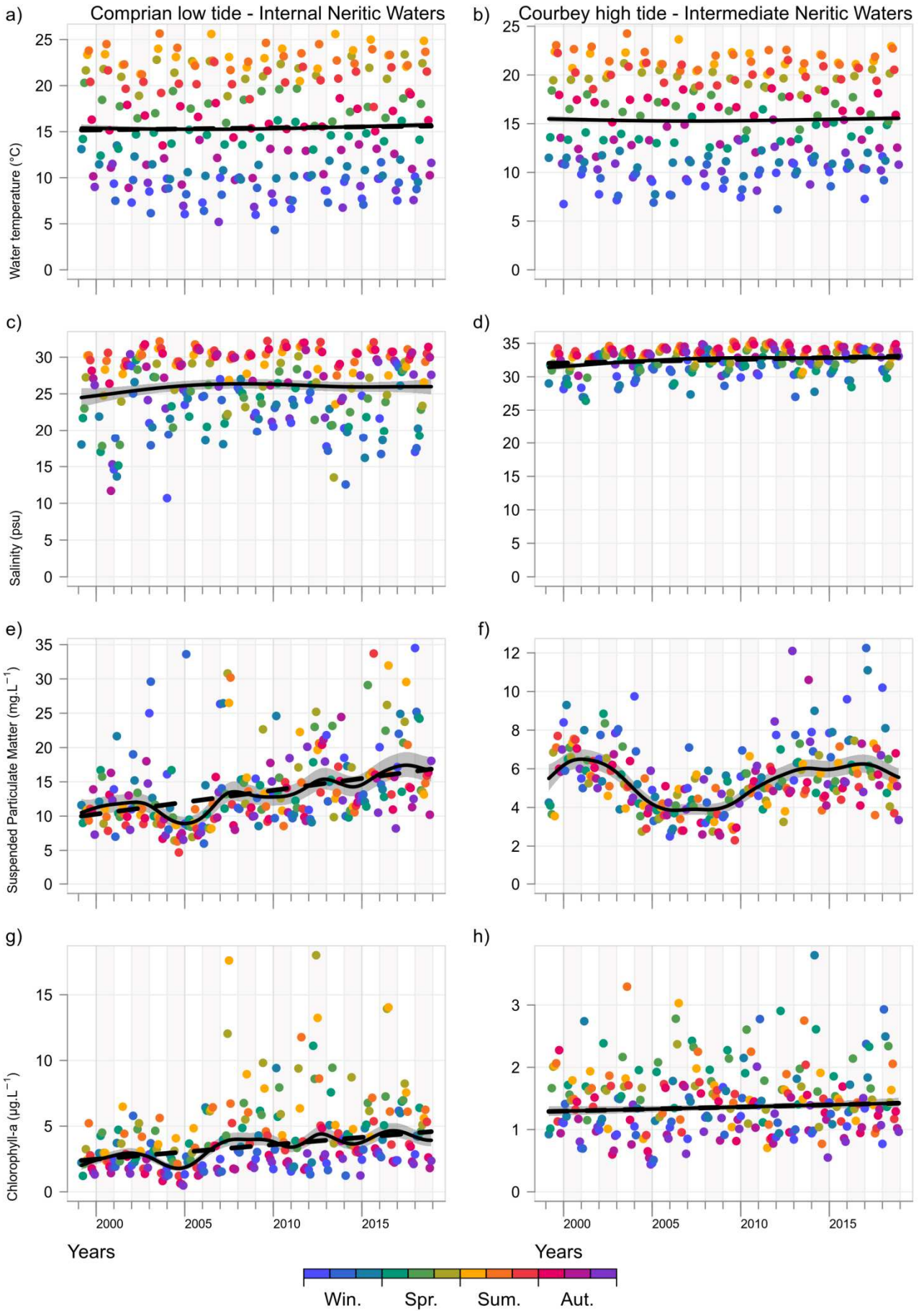


Figure 5: Bi-decadal inter-annual component of water temperature (a,b), salinity (c,d), suspended particulate

matter (e,f) and chlorophyll-a (g,h) at two contrasted stations (Comprian low tide (a, c, e, g) and Courbey high tide (b, d, f, h)) respectively representative of the inner and intermediate neritic waters in the Arcachon bay. In each panel, the plain black line is the DLM bi-decadal inter-annual component, the gray shadow is its confidence interval at 95%, the dots are the observations for each month coloured in function of the season. The bi-decadal changes were estimated with a modified Mann-Kendall test (Yue and Wang, 2004). When the test was significant, the Sen's line was drawn in dashed black.

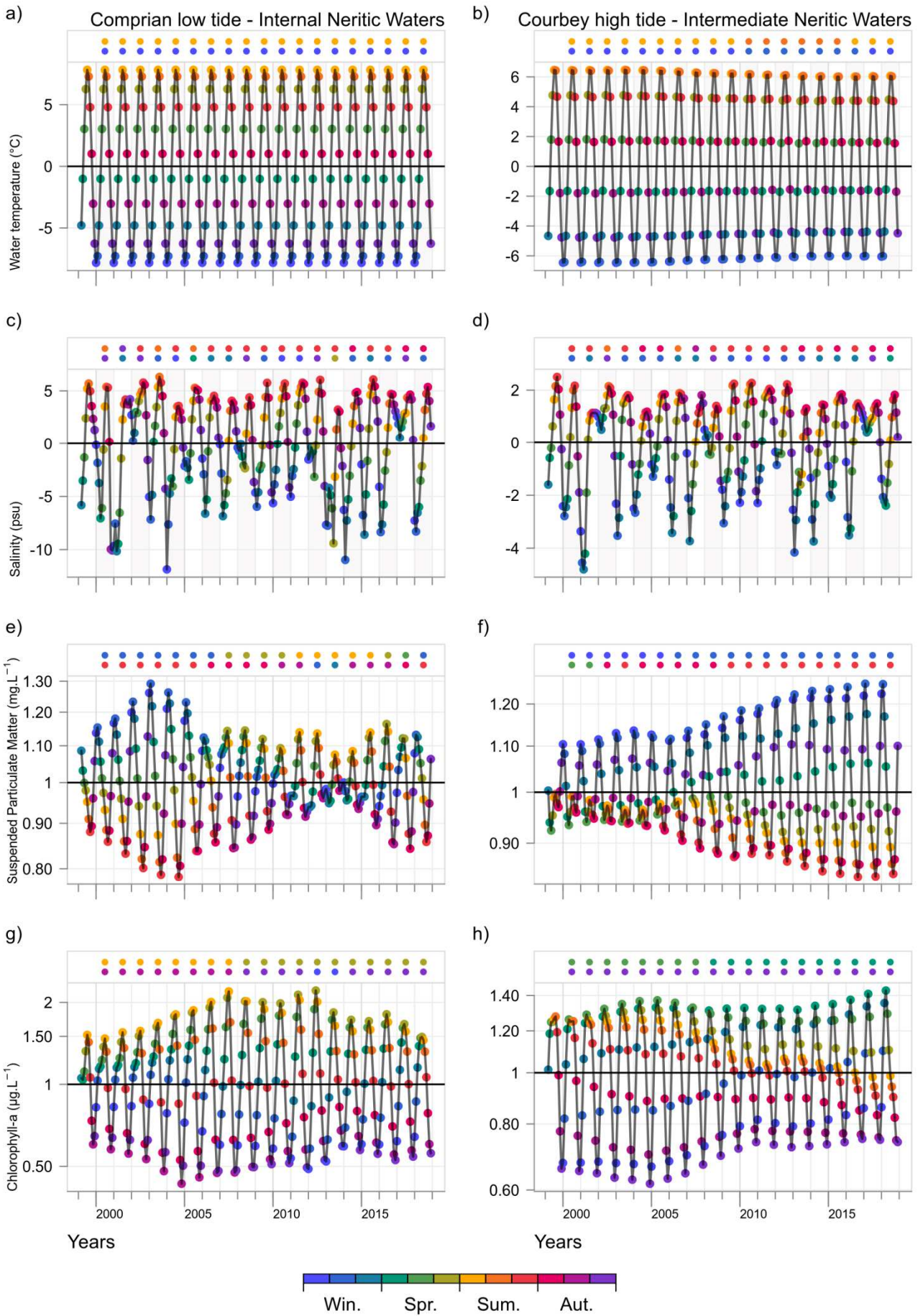


Figure 6: Bi-decadal seasonal components of water temperature (a,b), salinity (c,d), suspended particulate

matter (e,f) and chlorophyll-a (g,h) at two contrasted stations (Comprian low tide (a, c, e, g) and Courbey high tide (b, d, f, h)) respectively representative of the inner and intermediate neritic waters in the Arcachon bay. The dots are the DLM estimations for each month coloured in function of the season. When seasonal values equal to 0 (water temperature and salinity) or to 1 (suspended particulate matter and chlorophyll-a; horizontal black line), the fitted values were equal to the inter-annual component.

The dots at the top of each graph represent the month of maximum (top) and of minimum (bottom) of seasonality for each complete year.

449

450 **3.2.2. River parameters**

451 The Leyre discharge inter-annual component showed a strong inter-annual variability but
452 no significant increase nor decrease over the two decades (Figure 7a). The NO_x inter-
453 annual component also showed a strong inter-annual variability although less important
454 than the discharge rates (Figure 7c) No significant increase nor decrease were detected.
455 The NH₄⁺ inter-annual component showed no significant increase nor decrease although
456 two distinct periods occurred with an increase from 1999 to ca. 2007 and a decrease from
457 2008 to 2018 (Figure 7e). The SPM inter-annual component showed a significant
458 decrease in the Leyre River (Figure 7g).

459 The seasonal component amplitude of the river discharge, the maximal and minimal
460 values as well as their occurrence (seasonal maximum in winter/spring and minimum in
461 autumn) remained stable over the study period although they were characterised by a high
462 year-to-year variability (Figure 7b). The seasonal component amplitude of NO_x was higher
463 in the middle of the period resulting in a slight decrease of the maximal and minimal values
464 at the end of the period. The period of occurrence of the seasonal maximum remained
465 stable in late autumn / early winter, and the occurrence of the seasonal minimum was
466 delayed from summer to autumn (Figure 7d). The seasonal component amplitude of NH₄⁺
467 increased and was characterised by both an increase of the maximal and a decrease of
468 the minimal values. Except for the two first years, the occurrence of the seasonal
469 maximum remained stable in winter and the minimum was stable in autumn (Figure 7f).
470 The seasonal component amplitude of SPM increased with both an increase of the

471 maximal and a decrease of the minimal values but the occurrence of the seasonal
472 maximum and minimum remained stable in spring and autumn, respectively (Figure 7h).

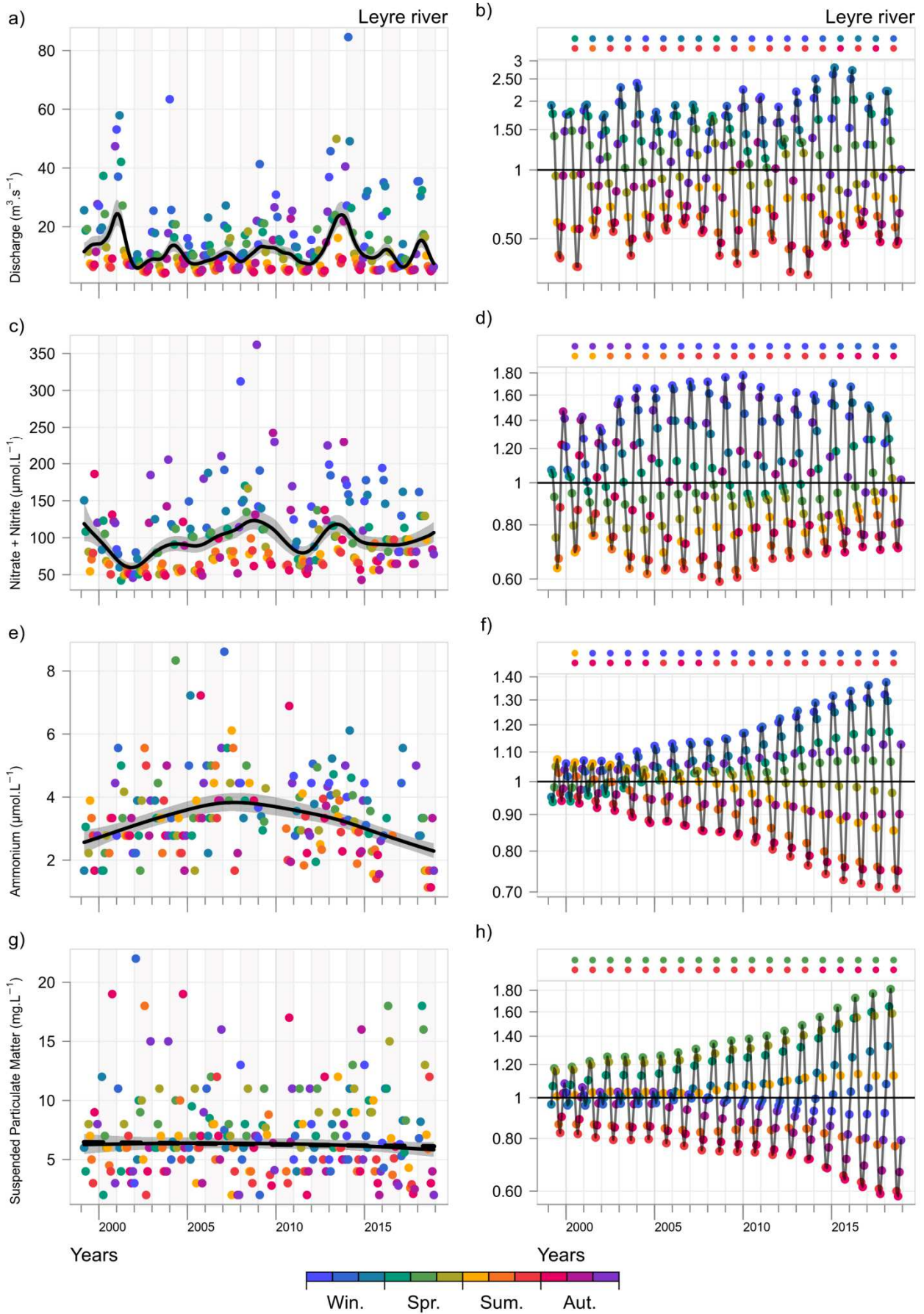


Figure 7: Bi-decadal inter-annual (a, c, e, g) and seasonality (b, d, f, h) components of river discharge (a,b),

nitrate + nitrite (c,d), ammonium (e,f) and suspended particulate matter (g,h) in the Leyre river. In the right hand side panels the plain black line is the DLM bi-decadal inter-annual component, the gray shadow its confidence interval at 90%, the dots are the observations for each month coloured in function of the season. In the left hand side panels the dots are the DLM estimations for each month coloured in function of the season. When seasonal values equal to 1 (horizontal black line), the fitted values were equal to the inter-annual component.

The bi-decadal changes were estimated with a modified Mann-Kendall (Yue and Wang, 2004). When the test was significant, the Sen's line was drawn in dashed black. At the top of each panel.

473

474 **3.2.3. Local climate**

475 The air temperature, irradiance, atmospheric pressure, and zonal component of the wind
476 did not show any trend whereas the wind intensity, meridional component of the wind and
477 monthly accumulated precipitation significantly decreased (Figure 8a, c, e, g, i, k, m). The
478 air temperature and irradiance seasonal component amplitude, seasonal maximal and
479 minimal values as well as their period of occurrence (seasonal maximum in summer and
480 minimum in winter and seasonal maximum in spring and minimum in autumn, respectively)
481 remained stable over the studied period (Figure 8b, d). The seasonal component
482 amplitude of the atmospheric pressure decreased over the studied period and was
483 characterised by a decrease of the maximal values. The period of occurrence of the
484 minima changed from summer to spring in 2005 whereas the occurrence of the maximum
485 always occurred in winter (Figure 8f). The seasonal component amplitude of the
486 accumulated rain increased over the studied period. It was characterised by both an
487 increase of the maximal and minimal values and the seasonal maximum and minimum
488 occurred in autumn and summer respectively (Figure 8h). The seasonal component
489 amplitude of the wind intensity increased and was characterised by both an increase in
490 maximal and minimal values. The period of occurrence of the seasonal maximum and
491 minimum remained stable in winter and summer respectively (Figure 8j). The seasonal
492 component amplitude of the zonal component of the wind decreased and was
493 characterised by the decrease of the maximal values and the increase of the minimal

494 values. The period of occurrence of the seasonal maximum changed from summer to
495 spring and the seasonal minimum remained in autumn (Figure 8l). The seasonal
496 component amplitude of the meridional component of the wind remained stable, as well as
497 the value and period of occurrence of the seasonal maximum (autumn) and minimum
498 (summer) (Figure 8n).

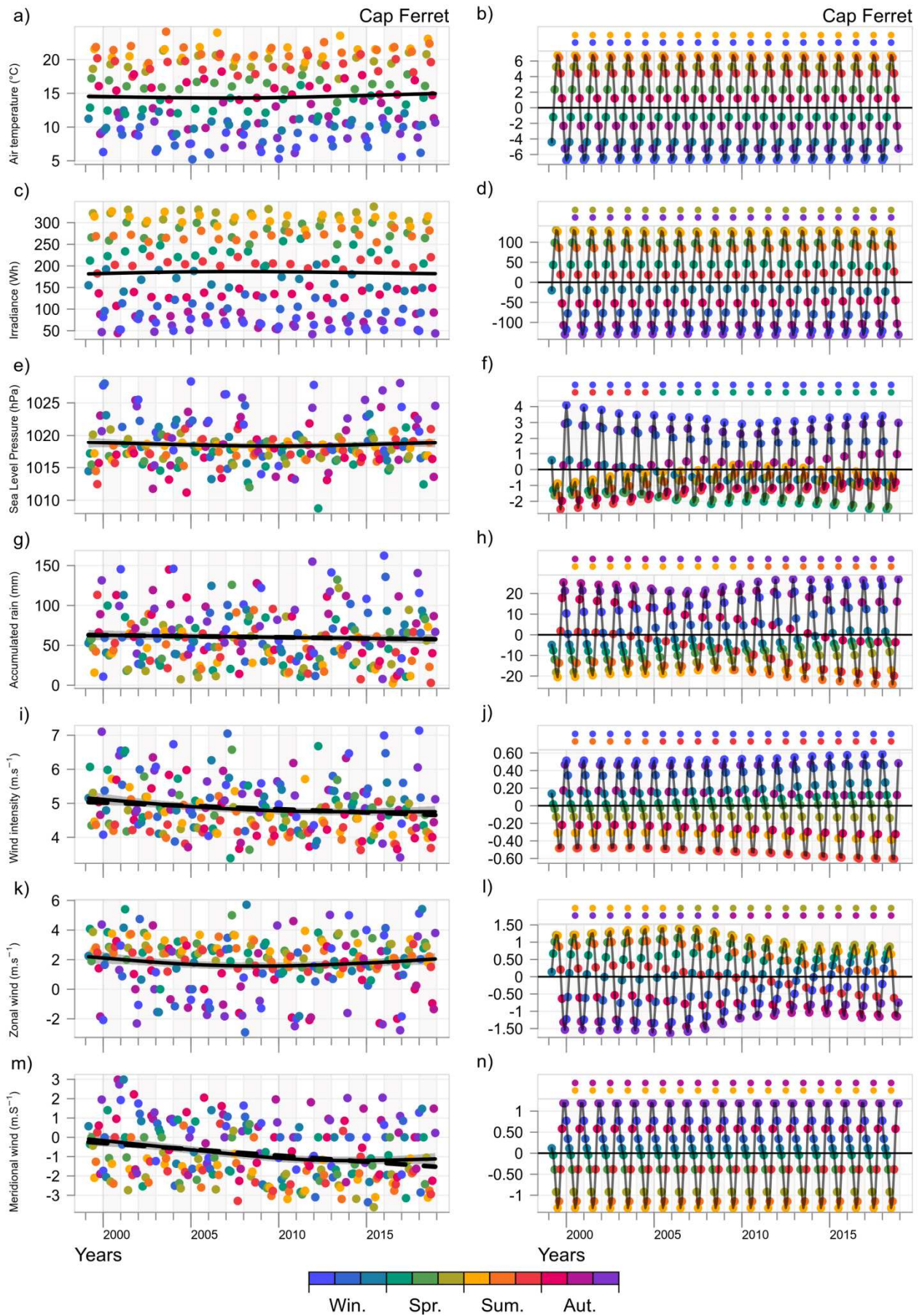


Figure 8: Bi-decadal inter-annual components (a, c, e, g, i, k, m) and seasonality (b, d, f, h, j, l, n) of air

temperature (a,b), irradiance (c,d), sea level pressure (e,f), monthly accumulated rain (g,h), wind intensity (i,j), zonal wind (k,l) and meridional wind (m,n) at Cap Ferret. In the right hand side panels the plain black line is the DLM bi-decadal inter-annual component, the gray shadow its confidence interval at 90%, the dots are the observations for each month coloured in function of the season. In the left hand side panels the dots are the DLM estimations for each month coloured in function of the season. When seasonal values equal to 0 (horizontal black line), the fitted values were equal to the inter-annual component.

The bi-decadal changes were estimated with a modified Mann-Kendall (Yue and Wang, 2004). When the test was significant, the Sen's line was drawn in dashed black. At the top of each panel.

499

500 3.3. Relationships between the nutrients and the abiotic drivers

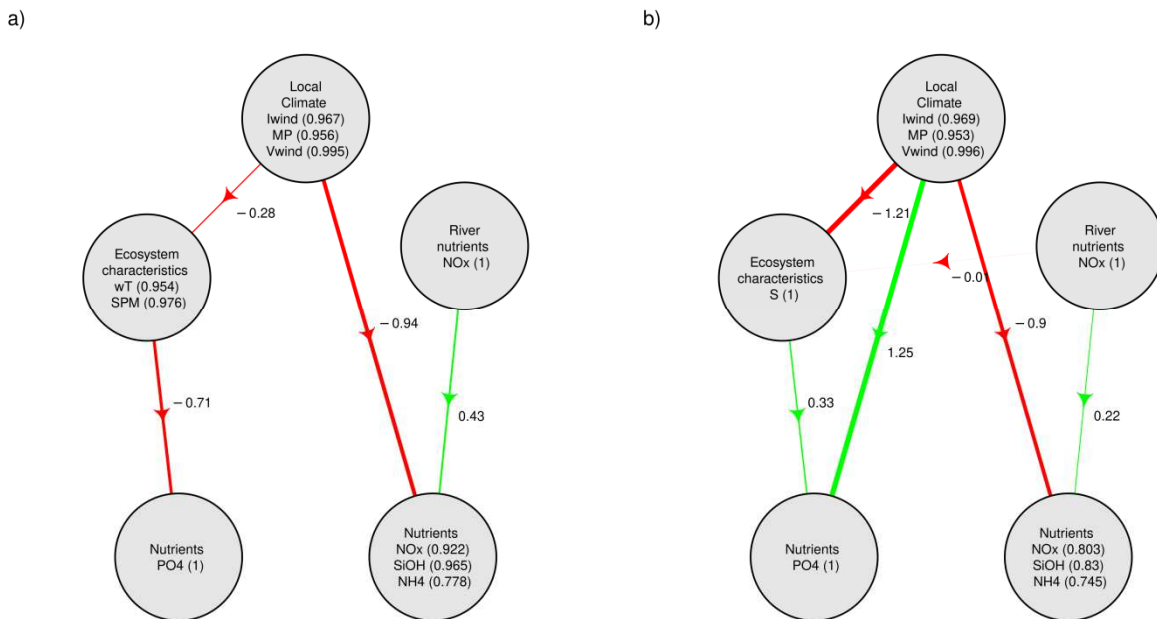


Figure 9: Relative influence of the potential drivers on the nutrients at Comprian LT (a) and Courbey HT (b). In each circle (latent variable; groups) are given and are followed by each manifest variable (parameter) and its loading (= correlation) to the latent variable. Green and red arrows represent positive and negative link respectively, with the associated path coefficient, the width of the arrow represents the strength of the relationship. Goodness of fit are 0.56 (a) and 0.62 (b).

501

502 Among the considered drivers, all groups but the Large scale climate had a significant
 503 direct and/or indirect influence on the bi-decadal inter-annual components of one or more
 504 nutrients (Figure 9). The Local climate always influenced a block of nutrients and was
 505 mostly expressed by wind and precipitations. At most stations, the NO_x, NH₄⁺ and Si(OH)₄
 506 group was more influenced by the River nutrients and the PO₄³⁻ by the Ecosystem

507 characteristics. The river influence on the N- and SI-nutrients was inversely proportional to
508 the distance to the river (stronger in the InNW and at low tide than in the ENW and at high
509 tide; Figure 9a, b). At most of the sites, the Ecosystem characteristics influence on the
510 PO_4^{3-} was expressed by the SPM at low tide and by salinity at high tide (Figure 9a, b).

511 **4. Discussion**

512 In the Arcachon bay, NO_x , NH_4^+ and $\text{Si}(\text{OH})_4$ concentrations increased in the beginning of
513 the twenty-first century whereas PO_4^{3-} concentrations decreased. These results were
514 inconsistent with results reported about other economically-developed countries. For
515 example, NO_x and organic phosphorus decreased in the lagoon of Venice (Sfriso et al
516 2019). In the bay of Seine, NO_x concentrations remained stable since 2007 and NH_4^+
517 concentration decreased since the 1990s (Romero et al., 2016). Other French ecosystems
518 also exhibited overall decreases of N- and Si-nutrients over the last two decades
519 (Lheureux et al., 2021). During the past decades, nutrients concentrations usually
520 decreased following the implementation of dams and the application of management
521 policies (Ragueneau et al., 2006).

522 Two categories of processes were investigated in order to explain the changes in nutrients
523 concentrations in the Arcachon Bay: (1) external nutrients inputs from adjacent
524 ecosystems and (2) internal processes occurring within the Arcachon bay.

525 **4.1 Changes in external drivers and consequences to nutrients**

526 *a) Leyre river inputs*

527 As in most temperate coastal ecosystems, N- and Si-nutrients in the Arcachon bay mainly
528 come from the rivers (Rimmelin et al., 1998). In this ecosystem, they mainly come from the
529 Leyre River (Canton et al., 2012), as illustrated by the combined nutrients and salinity
530 gradient from the internal to the external neritic waters (section 3.1.1; Table 2). Thus, any
531 increase or decrease of river nutrients concentrations and/or discharge would lead to any
532 subsequent change in nutrients concentrations in the bay as suggested by the results of
533 the PLS-PM (Figure 9).

534 There was no significant change in the river concentrations nor discharge (Figure 7) during
535 the two past decades. Thus, the bi-decadal increase in NO_x , NH_4^+ and Si(OH)_4
536 concentrations in the bay cannot be explained by changes in river input. The observed
537 relationship between river inputs and the nutrients in the Arcachon bay (section 3.1.1;
538 Figure 9) came from their similar inter-annual variability. In contrast to N- and Si-nutrients,
539 PO_4^{3-} did not mainly come from the Leyre River but from the sediment through
540 remineralisation and tidal pumping (Canton et al., 2012; Deborde et al., 2008; Delgard et
541 al., 2013; Glé et al. 2008; Plus et al., 2015). Thus, the Leyre River hypothesis does not
542 stand for PO_4^{3-} either.

543 In addition, there was no significant correlation between changes in nutrients
544 concentrations and changes in salinity, which can be considered as a proxy of freshwater
545 inputs. Therefore, the freshwater inputs were not suspected to having influenced the bi-
546 decadal nutrients changes in the bay.

547

548 *b) External drivers to flushing time*

549 An increase of the flushing time might lead to a decrease in nutrients export to the ocean
550 and thus an increase in nutrients retention and concentrations within the bay. Flushing
551 time is driven by the combination of freshwater inputs, residual currents, geomorphology,
552 and indirectly by wind conditions.

553 The wind and the river discharge were quantified as being of similar importance on the
554 Arcachon bay flushing time (Plus et al., 2009). In the Arcachon bay, because of its
555 geomorphology (the connection to the ocean is toward a narrow channel oriented along a
556 North-South axis), the meridional component of the wind is of interest. A decrease (or a
557 shift) in the South to North wind component would thus participate in an increase of the
558 flushing time (Plus et al., 2009) and consequently to a decrease of the nutrients retention

559 and concentrations within the bay (Figure 8). In addition, there was a negative relationship
560 between the meridional wind and the N- and Si-nutrients and, when any, positive with
561 PO_4^{3-} (Figure 9).

562 Thus, the wind was suspected to have an influence on the PO_4^{3-} changes in the Arcachon
563 bay although it cannot explain the increase in NO_x , NH_4^+ and Si(OH)_4 concentrations over
564 the past two decades.

565

566 c) Direct urban inputs

567 Compared to open bays, semi-enclosed bays are highly influenced by anthropogenic
568 activities due to their geomorphological characteristics (Peng et al., 2012). However, the
569 Arcachon bay might not struggle with such influence. Indeed, 151 thousand inhabitants
570 were living in the municipalities surrounding the Arcachon bay in 2019 (INSEE,
571 Populations légales en vigueur à compter du 1er janvier 2019) despite a 1.5-fold increase
572 during the study period. Both the population distribution and its increase were well
573 balanced between the Northern and Southern sides of the Arcachon bay.

574 Since the 1970's, the waste-water effluents are collected all around the bay, treated and
575 poured into the ocean at around 15 km at the South of the bay (Figure 1). As the long
576 shore wave direction is oriented southward (Idier et al., 2013), these effluents were thus
577 not likely to enter the bay. Therefore, urban effluents are not expected to have contributed
578 to the observed changes in nutrient concentrations within the bay due to the coupled
579 management actions were taken prior to the data collection and the regional water
580 circulation.

581

582 **4.2 Changes in internal processes and consequences to** 583 **nutrients**

584 *a) Direct influence of the seagrass decline*

585 As mentioned above, seagrass beds extent drastically declined in Arcachon bay between
586 1988 and 2007, with a sharp drop between 2005 and 2007, resulting in a decline of C
587 sequestration capacity as seagrass biomass from 25,000 to 16,500 ton C.y⁻¹ (Plus et al.,
588 2010; Ribaudou et al., 2016). Since that time, the seagrass beds have declined further and
589 winter biomasses are lower than in the past (Cognat, 2019)

590 Since these two species contain and take up N, P and Si, the seagrass meadows in the
591 Arcachon bay acts as a sink for nutrients (Wasserman et al., 1992; de Wit et al., 2005;
592 Plus et al., 2015 and references therein). Following the decline of the seagrass beds
593 extent, the *Z.noltei* nutrients consumption and N, P and Si stock capacity decreased.

594 The decrease in N and P uptake by the seagrass meadow was quantified at ca. 30%
595 between 2005 and 2009 (Plus et al., 2015). Si uptake decrease was not quantified but
596 probably followed the same pattern. The *Z. noltei* loss was particularly strong in the InNW
597 (Plus et al 2010), where the NH₄⁺ seasonality changed the most (Figure 3c). The period of
598 occurrence of the NH₄⁺ maxima values was advanced from January to October and the
599 minima from early summer to late spring (e.g. Figure 3c), suggesting a modification of the
600 biogeochemical processes in the Arcachon bay.

601 Clearly, a direct consequence of the decrease in *Z.noltei* biomass is its decrease in
602 nutrient uptake. This can explain the increase in NO_x, NH₄⁺ and Si(OH)₄ concentrations but
603 not the decrease in PO₄³⁻ concentration in the bay.

604

605 *b) Indirect influence of the seagrass decline*

606 The seagrass meadow plays a role in the sediment stability. Its action on the sediment
607 results in a more active particle trapping and storage (Ward et al., 1984), in a weakened
608 hydrodynamic pressure (Fonseca and Fisher, 1986) and finally in a reduction of particle
609 resuspension and an improvement of the water transparency. A reduction of the sediment
610 stability could enhance the sediment resuspension (Madsen et al., 2001) that
611 consequently enhances the inputs of benthic nutrients stored in the sediment pore water
612 into the water column (Wainright, 1990).

613 In the Arcachon bay, the decrease of the surface covered by *Z. noltei* altered the sediment
614 stability of tidal flats (Ganthy et al., 2011) and overall the sediment dynamics (Cognat,
615 2019). There was an increase in SPM during the study period (Table 3, Figure 5e) which
616 coincided in space with the decline of the seagrass meadow in the InNW (Figure 5e)
617 where a lot a seagrass patches disappeared (Plus et al., 2010). Thus, the decrease of the
618 surface covered by *Z. noltei* had likely increased the advection of benthic nutrients to the
619 water column. In addition, the nutrients flux from the sediment to the water column is
620 higher in bare sediments than in vegetated sediments in the Arcachon bay (Delgard et al.,
621 2013). Consequently, the decrease of the seagrass meadow induced an increase of the
622 nutrients concentrations in the water column through the enhancement of the nutrient flux
623 from the sediment to the water column. Again, this can explain the increase in NO_x , NH_4^+
624 and $\text{Si}(\text{OH})_4$ concentrations but not the decrease in PO_4^{3-} concentration in the bay.

625 In oxic conditions like in the Arcachon bay, PO_4^{3-} ion has the property of adsorbing onto
626 the particles (Froelich et al., 1988). Consequently, an increase in SPM concentration could
627 enhance the PO_4^{3-} adsorption and consequently decrease the PO_4^{3-} concentration in the
628 dissolved phase, as seen at Comprian LT, Girouasse LT and Tès LT (Table 2 and 3;
629 Figures 2e, 5e, 9a and Supplementary Material A). However, the capacity of resuspended
630 sediment particles to adsorb water column PO_4^{3-} partly depends on the (under)saturation
631 of the adsorption sites of the particles. In the absence of information regarding the

632 saturation state of these sites, the influence of resuspended sediment on the PO_4^{3-}
633 concentration in the Arcachon bay cannot be assessed.

634 *c) Complementary physical influence*

635 Water temperature increased significantly at many stations (Table 3). An increase in
636 temperature could increase the remineralisation processes and the benthic flux of nutrients
637 to water column in muddy sediments (Nowicki & Nixon 1985), thus favouring an increase
638 in remineralised-nutrients (NH_4^+ , PO_4^{3-} , $\text{Si}(\text{OH})_4$) concentrations in the water column. Also,
639 an *in-situ* experiment revealed that an increase in ambient temperature could increase the
640 PO_4^{3-} adsorption to the sediment (Zhang and Huang, 2011). Thus, the increase in water
641 temperature may have contributed to the increase of the concentrations in NH_4^+ , PO_4^{3-} ,
642 $\text{Si}(\text{OH})_4$ and may have concurrently decreased PO_4^{3-} concentration in the Arcachon bay.

643

644 *d) Biotic compartment: influence of phytoplankton*

645 It was assumed that the seagrass decline has led to an increase in nutrients
646 concentrations in the Arcachon bay. Phytoplankton, as all primary producer, has a tight
647 relationship with nutrients since nutrients are mandatory for their growth. Chlorophyll-*a*
648 concentration increased during the study period (Table 3; Figure 5g, h; Supplementary
649 Material A) suggesting an increase in phytoplankton biomass, increase probably due to the
650 concomitant increase in nutrients concentrations. However, the response of N-nutrients
651 and $\text{Si}(\text{OH})_4$ (increase) to the seagrass decrease and to the phytoplankton increase was
652 opposed to the PO_4^{3-} response (decrease). This may be explained by the higher N:P:Si
653 ratios for *Z. noltei* than for phytoplankton: *Z. noltei* N:P ratio and Si:P ratio range between
654 15 and 35 mol mol⁻¹ (Brun et al., 2002; Plus et al., 2006) and between 25 and 80 mol mol⁻¹
655 (Wasserman et al., 1992), respectively, whereas the reference value of phytoplankton
656 N:P:Si ratios is 16:1:16 mol mol⁻¹ (Harrison et al., 1977). This indicates that, for a given

657 need in N and Si, the need in P is higher for the phytoplankton (which is essentially
658 diatom-dominated, Glé et al. 2008) than for *Z. noltei*.

659 At the beginning of the study period in the Arcachon bay, the phytoplankton was potentially
660 more often limited by N (N:P:Si ratio < 16:1:16) during most of the production period
661 (Figure 4, Supplementary material C). Thus, the increase in N (and Si) availability due to
662 the seagrass decline has led to the increase in phytoplankton biomass. Because the need
663 in P (for a given need in N and Si) is higher for the phytoplankton than for *Z. noltei*, the
664 increase in phytoplankton biomass have favoured the decrease in PO_4^{3-} concentration.
665 Consequently, along the study period, the potential nutrient-limitation has switched from N
666 to P during the phytoplankton production period (Figure 4, Supplementary material C).
667 Depending on the site, the potential P-limitation occurred during most or during all the
668 phytoplankton production period.

669 To summarize, the increase in NO_x and $\text{Si}(\text{OH})_4$ concentrations may have supported the
670 phytoplankton biomass that have concurrently favoured the PO_4^{3-} decrease in the bay.

671

672 e) Biotic compartment: influence of fauna

673 In coastal ecosystems, benthic primary consumers have two main direct and indirect
674 influence on nutrients. First, filter feeders consume phytoplankton as a main trophic
675 resource (Kaspar et al., 1985); thus, they extract organic matter from the water column
676 preventing its export to the ocean, they transform it into benthic biomass and then transfer
677 it to the sediment as faeces and pseudo-faeces (Lindström Swanberg, 1991). Therefore,
678 filter feeders contribute to maintain nutrients within the coastal ecosystems by enhancing
679 the intra-ecosystem organic material recycling into nutrients (Kaspar et al., 1985; Dame
680 and Dunkers 1988), especially in well-mixed shallow systems Del Amo et al. 1997).
681 Second, benthic species can stimulate benthic algal productivity and bioturbation

682 processes, thus enhancing the benthic nutrient release (Lindström Swanberg, 1991).
683 Concerning the pelagic realm, zooplankton also participates to the nutrient
684 remineralisation through organic matter feeding and excretion.

685 In the Arcachon bay, the estimated stock of benthos was around 100 kt. This included
686 around 17 kt of the cultivated oyster *Crassostrea gigas* and 65 kt of wild oysters, in 2009
687 and 2011 respectively (Scourzic et al., 2012); around 2kt of the Manila clam *Ruditapes*
688 *philippinarum* (Sanchez et al., 2018); around 0.4 kt of the cockle *Cerastoderma edule*
689 (calculated from Blanchet (2004) and Ricciardi and Bourget (1998)); around 0.32 kt of the
690 crepidula *Crepidula fornicata* in 2011 (de Montaudouin et al., 2018) and around 15 kt of
691 other species (calculated from Blanchet (2004) and Ricciardi and Bourget (1998)).
692 *Cerastoderma edule* and *Crepidula fornicata* biomasses increased during the study period
693 but they were not considered having an influence on the nutrients regarding their very low
694 biomasses. *Ruditapes philippinarum* biomass remained similar between 2003 and 2018.
695 Although the stock of cultivated oysters decreased between the end of the twentieth
696 century and 2009 (Scourzic et al., 2012), there is unfortunately no information regarding
697 the wild oysters stock changes (H. Blanchet and X. de Montaudouin, pers. com.).

698 Thus, it would be speculative to consider a major influence of these species on the
699 nutrients but one can consider that the oysters being the major compartment, their
700 biomass changes might drive the bivalve species influence on the nutrients. If the wild
701 oysters biomass had increased, it might have induced an increase in the trapping of
702 phytoplankton and its direct remineralisation into nutrients, directly or through the bacterial
703 remineralisation of faeces and pseudo-faeces; and thus it might have contributed to the
704 increase in N- and Si- nutrient concentrations in the Arcachon bay avoiding its flush out of
705 the system through tidal turnover. If the wild oysters biomass had decreased, the inverse
706 processes were expected.

707

708 **4.3 Synthesis of the nutrient changes and perspectives**

709 Upon these hypotheses, it appeared that nutrients changes in the Arcachon bay principally
710 resulted from internal processes, and that most of them were linked. The seagrass
711 meadow decline was at the centre of our explanation as it was involved in most of the
712 processes (Figure 10).

713 First, less nutrients were consumed by seagrasses, leaving more available nutrients in the
714 water column. These newly available nutrients supported an increase of the phytoplankton
715 biomass that participated in the change in nutrient ratios: the higher phytoplankton need in
716 P than the *Z. noltei* (for a given need in N and Si) shifted the main potential limitation of
717 phytoplankton production from N to P. This phytoplankton biomass increase triggered the
718 P depletion when NO_x , NH_4^+ and $\text{Si}(\text{OH})_4$ increased.

719 Second, the decrease of surface covered by the seagrass meadows increased bare
720 sediment surface, leading to a rise of both sediments and nutrients fluxes from the bed to
721 the water column. However, the impacts of resulting higher SPM concentrations on PO_4^{3-}
722 concentrations (through sorption processes) could not be assessed yet.

723 Finally, despite the increase in water temperature that probably might have had a
724 synergistic effect on the enhancement of remineralisation, the observed wind direction
725 changes, through their influence on the flushing time, could have contributed to the
726 decrease in PO_4^{3-} concentrations.

727 Many studies described the (pluri-)decadal bottom-up control of nutrient concentration on
728 primary producers and even on higher trophic levels (Carpenter and Kitchell, 1993;
729 Derolez et al., 2019, 2020; Sand-Jensen et al., 2017). The present study illustrates on the
730 one hand the top-down control of primary producers on the nutrients concentrations and
731 stoichiometry, and on the other hand the competition between primary producers through
732 their resource in nutrient. Specifically, the study highlights the major role of the seagrass

733 meadow on the bi-decadal changes in nutrients concentrations and ratios, and indirectly
734 on phytoplankton biomass, in the Arcachon bay. The potential nutrient limitation of the
735 phytoplankton growth changed during the studied period due to more available nutrients
736 but different relative uptake needs between phytoplankton and *Zostera*. Other studies
737 found that changes in phytoplankton specific and functional diversity were related to
738 changes in sediment resuspension — as microphytobenthos is related to sediment
739 dynamics (Lucas et al., 2000) — or to climatic and climate-driven physical factors (David et
740 al. ,2012; Hernández-Fariñas et al. ,2014).

741 Thus, the seagrass meadow might not have had a direct and/or indirect influence only on
742 the phytoplankton biomass but also on its community structure. It would therefore be
743 interesting to study the long-term changes in nutrient ratios, which seem to be important in
744 the ecosystems functioning changes, in relation to phytoplankton community changes. It
745 would also be interesting to put into perspective the patent influence of local processes in
746 the Arcachon bay functioning by including it in a multi-ecosystemic study. Indeed, some
747 studies revealed the influence of large-scale climate onto physico-biogeochemical
748 parameters (including nutrients; Goberville et al. (2010), Lheureux et al. (2021)) and onto
749 phytoplankton communities (David et al. (2012), Hernández-Fariñas et al. (2014)). One
750 question would be: at multi-ecosystem scale, do changes in nutrient concentrations and
751 ratios in coastal ecosystems mainly respond to changes in local or in large-scale drivers?

758 the research project EVOLECO-vφ (LEFE-CYBER). Data sets regarding the drivers were
759 provided by NOAA, NCEP/NCAR, MeteoFrance, EauFrance and the different French
760 Water Agencies. We also thank all members of these different institutions, from the field
761 workers and analysts to the coordinators, who made the use of the data possible.

762

763 **CRedit author statement**

764 Study design: AL, VD, YdA, NS. Data collection, either on the field or in the lab, and/or to
765 the data analysis: AL, VD, YdA, DS, IA, HB, MAC, LC, SF, LM, AN, MP, FDA, FG, LG, CM,
766 HOJ, LR, MR, MPT, FT, GT, NS. Writing: AL, VD, YdA, NS. Writing-reviewing and editing:
767 VD, YdA, DS, IA, HB, FG, NS.

768 **References**

- 769 Auby, I., Manaud, F., Maurer, D., Trut, G., 1994. Étude de la prolifération des algues vertes
770 dans le bassin d’Arcachon. Ifremer, Cemagref, SSA, SABARC 292.
- 771 Barnston, A.G., Livezey, R.E., 1987. Classification, Seasonality and Persistence of Low-
772 Frequency Atmospheric Circulation Patterns. *Mon. Weather Rev.*
773 [https://doi.org/10.1175/1520-0493\(1987\)115<1083:CSAPOL>2.0.CO;2](https://doi.org/10.1175/1520-0493(1987)115<1083:CSAPOL>2.0.CO;2)
- 774 Belin, C., Soudant, D., Amzil, Z. 2021. Three decades of data on phytoplankton and
775 phycotoxins on the French coast: Lessons from REPHY and REPHYTOX. *Harmful*
776 *Algae* 102, 101733. <https://doi.org/10.1016/j.hal.2019.101733>
- 777 Beusen, A.H.W., Bouwman, A.F., Beek, L.P.H. Van, Mogollón, J.M., Middelburg, J.J., 2016.
778 Global riverine N and P transport to ocean increased during the 20th century despite
779 increased retention along the aquatic continuum 2441–2451.
780 <https://doi.org/10.5194/bg-13-2441-2016>
- 781 Blanchet, H., 2004. Structure et Fonctionnement des Peuplements Benthiques du Bassin
782 d’Arcachon. Université de Bordeaux.
- 783 Borum, J., Sand-Jensen, K., 1996. Is Total Primary Production in Shallow Coastal Marine
784 Waters Stimulated by Nitrogen Loading? *Oikos* 76, 406.
785 <https://doi.org/10.2307/3546213>

- 786 Bouchet, J.M., 1968. Etude océanographique des chenaux du bassin d'Arcachon. Thèse
787 d'état, Université de Bordeaux , France.
- 788 Bouwman, A.F., Bierkens, M.F.P., Griffioen, J., Hefting, M.M., Middelburg, J.J.,
789 Middelkoop, H., Slomp, C.P., 2013. Nutrient dynamics, transfer and retention along the
790 aquatic continuum from land to ocean: Towards integration of ecological and
791 biogeochemical models. *Biogeosciences* 10, 1–23. [https://doi.org/10.5194/bg-10-1-](https://doi.org/10.5194/bg-10-1-2013)
792 2013
- 793 Box GEP, Jenkins GW (1976) Time series analysis: forecasting and control, Holden-
794 Day. San Francisco, CA.
- 795 Buestel, D., Ropert, M., Prou, J., Gouletquer, P., 2009. History, status, and future of oyster
796 culture in France. *J. Shellfish Res.* 28, 813–820. <https://doi.org/10.2983/035.028.0410>
797
- 798 Caill-Milly, N., Bobinet , J., Lissardy, M., Morandeau, G, Sanchez, F. 2008. Campagne
799 d'évaluation du stock de palourdes du bassin d'Arcachon - Année 2008.
- 800
801 Canton, M., Anschutz, P., Coynel, A., Polsenaere, P., Auby, I., Poirier, D., 2012. Nutrient
802 export to an Eastern Atlantic coastal zone: First modeling and nitrogen mass balance.
803 *Biogeochemistry* 107, 361–377. <https://doi.org/10.1007/s10533-010-9558-7>
- 804 Carpenter S.R. and Kitchell J.F., 1993. The trophic cascade in lakes. Cambridge
805 University Press, Cambridge.
806
- 807 Chatfield, C (1996) The analysis of time series: an introduction, Chapman&Hall. London.
808
- 809 Chelton, DB (1984) Commentary: short-term climatic variability in the northeast Pacific
810 Ocean. In: *The influence of ocean conditions on the production of salmonids in the*
811 *North Pacific*. Percy W (ed) Corvallis, OR, Oregon State University Press, p 87–99
812
- 813 Christiansen, C., Vølund, G., Lund-Hansen, L.C., Bartholdy, J., 2006. Wind influence on
814 tidal flat sediment dynamics: Field investigations in the Ho Bugt, Danish Wadden Sea.
815 *Mar. Geol.* 235, 75–86. <https://doi.org/10.1016/j.margeo.2006.10.006>
- 816 Cloern, J.E., 2001. Our evolving conceptual model of the coastaleutrophication problem.
817 *Mar Ecol Prog Ser Natl. Res. Counc.* 210, 223–253.
- 818 Cloern, J.E., Jassby, A.D., Thompson, J.K., Hieb, K.A., 2007. A cold phase of the East
819 Pacific triggers new phytoplankton blooms in San Francisco Bay. *Proc. Natl. Acad.*
820 *Sci. U. S. A.* 104, 18561–18565.
- 821 Cloern, J.E., Hieb, K.A., Jacobson, T., Sansó, B., Di Lorenzo, E., Stacey, M.T., Largier,
822 J.L., Meiring, W., Peterson, W.T., Powell, T.M., Winder, M., Jassby, A.D., 2010.
823 Biological communities in San Francisco Bay track large-scale climate forcing over the
824 North Pacific. *Geophys. Res. Lett.* 37, L21602.
825 <http://dx.doi.org/10.1029/2010GL044774>
- 826 Cocquempot, L., Delacourt, C., Paillet, J., Riou, P., Aucan, J., Castelle, B., Charria, G.,
827 Claudet, J., Conan, P., Coppola, L., Hocdé, R., Planes, S., Raimbault, P., Savoye, N.,
828 Testut, L., Vuillemin, R., 2019. Coastal ocean and nearshore observation: A French
829 case study. *Front. Mar. Sci.* 6, 1–17. <https://doi.org/10.3389/fmars.2019.00324>

- 830 Cognat, M., 2019. Rôles des facteurs environnementaux et des interactions
831 biomorphologiques sur l'évolution spatio-temporelle des herbiers de zostères dans
832 une lagune mésotidale. Université de Bordeaux.
- 833 Conley, D.J., 2002. Terrestrial ecosystems and the global biogeochemical silica cycle.
834 *Global Biogeochem. Cycles* 16, 68-1-68–8. <https://doi.org/10.1029/2002gb001894>
- 835 Dame, R.F., Dankers, N., 1988. Uptake and release of materials by a Wadden sea mussel
836 bed. *J. Exp. Mar. Bio. Ecol.* 118, 207–216. [https://doi.org/10.1016/0022-0981\(88\)90073-1](https://doi.org/10.1016/0022-0981(88)90073-1)
- 838 David, V., Ryckaert, M., Karpytchev, M., Bacher, C., Arnaudeau, V., Vidal, N., Maurer, D.,
839 Niquil, N., 2012. Estuarine , Coastal and Shelf Science Spatial and long-term changes
840 in the functional and structural phytoplankton communities along the French Atlantic
841 coast. *Estuar. Coast. Shelf Sci.* 1–15. <https://doi.org/10.1016/j.ecss.2012.02.017>
- 842 De Montaudouin, X., Blanchet, H., Hippert, B., 2018. Relationship between the invasive
843 slipper limpet *Crepidula fornicata* and benthic megafauna structure and diversity, in
844 Arcachon Bay. *J. Mar. Biol. Assoc. United Kingdom* 98, 2017–2028.
845 <https://doi.org/10.1017/S0025315417001655>
- 846 De Wit, R., Leibreich, J., Vernier, F., Delmas, F., Beuffe, H., Maison, P., Chossat, J.C.,
847 Laplace-Treytore, C., Laplana, R., Clavé, V., Torre, M., Auby, I., Trut, G., Maurer, D.,
848 Capdeville, P., 2005. Relationship between land-use in the agro-forestry system of les
849 Landes, nitrogen loading to and risk of macro-algal blooming in the Bassin d’Arcachon
850 coastal lagoon (SW France). *Estuar. Coast. Shelf Sci.* 62, 453–465.
851 <https://doi.org/10.1016/j.ecss.2004.09.007>
- 852 Deborde, J., Abril, G., Mouret, A., Jézéquel, D., Thouzeau, G., Clavier, J., Bachelet, G.,
853 Anschutz, P., 2008. Effects of seasonal dynamics in a *Zostera noltei* meadow on
854 phosphorus and iron cycles in a tidal mudflat (Arcachon Bay, France). *Mar. Ecol.*
855 *Prog. Ser.* 355, 59–71. <https://doi.org/10.3354/meps07254>
- 856 Delgard, M.L., Deflandre, B., Deborde, J., Richard, M., Charbonnier, C., Anschutz, P.,
857 2013. Changes in Nutrient Biogeochemistry in Response to the Regression of *Zostera*
858 *noltei* Meadows in the Arcachon Bay (France). *Aquat. Geochemistry* 19, 241–259.
859 <https://doi.org/10.1007/s10498-013-9192-9>
- 860 Derolez, V., Bec, B., Munaron, D., Fiandrino, A., Pete, R., Simier, M., Souchu, P., Laugier,
861 T., Aliaume, C., Malet, N., 2019. Recovery trajectories following the reduction of urban
862 nutrient inputs along the eutrophication gradient in French Mediterranean lagoons.
863 *Ocean Coast Manage* 171, 1–10. <https://doi.org/10.1016/j.ocecoaman.2019.01.012>
- 864 Derolez, V., Malet, N., Fiandrino, A., Lagarde, F., Richard, M., Ouisse, V., Bec, B.,
865 Aliaume, C., 2020. Fifty years of ecological changes: Regime shifts and drivers in a
866 coastal Mediterranean lagoon during oligotrophication. *Sci Total Environ* 732, 139292.
867 <https://doi.org/10.1016/j.scitotenv.2020.139292>
- 868 Doney, S.C., 2006. Oceanography: Plankton in a warmer world. *Nature* 444, 695–696.
869 <https://doi.org/10.1038/444695a>
- 870
- 871 Duarte, C.M., Conley, D.J., Cartensen, J., Sánchez-Camacho, M., 2008. Return to
872 *Neverland*: Shifting Baselines Affect Eutrophication Restoration Targets. *Estuaries*
873 *Coasts* 32, 29–36. <http://doi.org/10.1007/s12237-008-9111-2>

- 874 Durrieu de Madron, X., Guieu, C., Sempéré, R., Conan, P., Cossa, D., D'Ortenzio, F.,
875 Estournel, C., Gazeau, F., Rabouille, C., Stemmann, L., Bonnet, S., Diaz, F., Koubbi,
876 P., Radakovitch, O., Babin, M., Baklouti, M., Bancon-Montigny, C., Belviso, S.,
877 Bensoussan, N., Bonsang, B., Bouloubassi, I., Brunet, C., Cadiou, J.F., Carlotti, F.,
878 Chami, M., Charmasson, S., Charrière, B., Dachs, J., Doxaran, D., Dutay, J.C., Elbaz-
879 Poulichet, F., Eléaume, M., Eyrolles, F., Fernandez, C., Fowler, S., Francour, P.,
880 Gaertner, J.C., Galzin, R., Gasparini, S., Ghiglione, J.F., Gonzalez, J.L., Goyet, C.,
881 Guidi, L., Guizien, K., Heimbürger, L.E., Jacquet, S.H.M., Jeffrey, W.H., Joux, F., Le
882 Hir, P., Leblanc, K., Lefèvre, D., Lejeusne, C., Lemé, R., Loÿe-Pilot, M.D., Mallet, M.,
883 Méjanelle, L., Mélin, F., Mellon, C., Mérigot, B., Merle, P.L., Migon, C., Miller, W.L.,
884 Mortier, L., Mostajir, B., Mousseau, L., Moutin, T., Para, J., Pérez, T., Petrenko, A.,
885 Poggiale, J.C., Prieur, L., Pujo-Pay, M., Pulido-Villena, Raimbault, P., Rees, A.P.,
886 Ridame, C., Rontani, J.F., Ruiz Pino, D., Sicre, M.A., Taillandier, V., Tamburini, C.,
887 Tanaka, T., Taupier-Letage, I., Tedetti, M., Testor, P., Thébault, H., Thouvenin, B.,
888 Touratier, F., Tronczynski, J., Ulses, C., Van Wambeke, F., Vantrepotte, V., Vaz, S.,
889 Verney, R., 2011. Marine ecosystems' responses to climatic and anthropogenic
890 forcings in the Mediterranean. *Prog. Oceanogr.* 91, 97–166.
891 <https://doi.org/10.1016/j.pocean.2011.02.003>
- 892 Enfield, D.B., Mestas-Nuñez, A.M., Trimble, P.J., 2001. The Atlantic multidecadal
893 oscillation and its relation to rainfall and river flows in the continental U.S. *Geophys.*
894 *Res. Lett.* 28, 2077–2080. <https://doi.org/10.1029/2000GL012745>
- 895 Fonseca, M.S., Fisher, J.S., 1986. A comparison of canopy friction and sediment
896 movement between four species of seagrass with reference to their ecology and
897 restoration. *Mar. Ecol. Prog. Ser.* 29, 15–22. [https://doi.org/10.1016/S0300-9629\(76\)80020-5](https://doi.org/10.1016/S0300-9629(76)80020-5)
- 899 Froelich, P.N., 1988. Kinetic control of dissolved phosphate in natural rivers and estuaries:
900 A primer on the phosphate buffer mechanism. *Limnol. Oceanogr.* 33, 649–668.
901 <https://doi.org/10.4319/lo.1988.33.4part2.0649>
- 902 Galloway, J.N., Dentener, F.J., Capone, D.G., Boyer, E.W., Howarth, R.W., Seitzinger, S.P.,
903 Asner, G.P., Cleveland, C.C., Green, P.A., Holland, E.A., Karl, D.M., Michaels, A.F.,
904 Porter, J.H., Townsend, A.R., Vörösmarty, C.J., 2004. Nitrogen cycles: Past, present,
905 and future, *Biogeochemistry*. <https://doi.org/10.1007/s10533-004-0370-0>
- 906 Ganthy, F., Sottolichio, A., Verney, R., 2011. The stability of vegetated tidal flats in a
907 coastal lagoon through quasi in-situ measurements of sediment erodibility. *J. Coast.*
908 *Res.* 1500–1504.
- 909 Gelaro, R., McCarty, W., Suárez, M.J., Todling, R., Molod, A., Takacs, L., Randles, C.A.,
910 Darmenov, A., Bosilovich, M.G., Reichle, R., Wargan, K., Coy, L., Cullather, R.,
911 Draper, C., Akella, S., Buchard, V., Conaty, A., da Silva, A.M., Gu, W., Kim, G.K.,
912 Koster, R., Lucchesi, R., Merkova, D., Nielsen, J.E., Partyka, G., Pawson, S., Putman,
913 W., Rienecker, M., Schubert, S.D., Sienkiewicz, M., Zhao, B., 2017. The modern-era
914 retrospective analysis for research and applications, version 2 (MERRA-2). *J. Clim.*
915 30, 5419–5454. <https://doi.org/10.1175/JCLI-D-16-0758.1>
- 916 Glé, C., Del Amo, Y., Sautour, B., Laborde, P., Chardy, P., 2008. Variability of nutrients and
917 phytoplankton primary production in a shallow macrotidal coastal ecosystem
918 (Arcachon Bay, France). *Estuar. Coast. Shelf Sci.* 76, 642–656.
919 <https://doi.org/10.1016/j.ecss.2007.07.043>

- 920 Goberville, E., Beaugrand, G., Sautour, B., Tréguer, P., 2010. Climate-driven changes in
921 coastal marine systems of western Europe. *Mar. Ecol. Prog. Ser.* 408, 129–147.
922 <https://doi.org/10.3354/meps08564>
- 923 Goldfeld, S.M., Quandt, R.E., 1965. Some Tests for Homoscedasticity. *J. Am. Stat. Assoc.*
924 60, 539–547. <https://doi.org/10.1080/01621459.1965.10480811>
- 925 Harding, L.W., Gallegos, C.L., Perry, E.S., Miller, W.D., Adolf, J.E., Mallonee, M.E., Paerl,
926 H.W., 2016. Long-Term Trends of Nutrients and Phytoplankton in Chesapeake Bay.
927 *Estuaries and Coasts* 39, 664–681. <https://doi.org/10.1007/s12237-015-0023-7>
- 928 Harrison, P.J., Conway, H.L., Holmes, R.W., Davis, C.O., 1977. Marine Diatoms in
929 Chemostats under Silicate or Ammonium Limitation. III. Cellular Chemical
930 Composition and Morphology of *Chaetoceros debilis*, *Skeletonema costatum*, and
931 *Thalassiosira gravida**. *Mar. Biol.* 43, 19–31.
- 932 Helsel, D.R., Hirsch, R.M., 1992. Statistical methods in water resources, in: *Techniques of*
933 *Water-Resources Investigations of the United States Geological Survey Book 4,*
934 *Hydrologic Analysis and Interpretation.* <https://doi.org/10.2307/1269385>
- 935 Hernández-Fariñas, T., Soudant, D., Barillé, L., Belin, C., Lefebvre, A., Bacher, C., 2014.
936 Temporal changes in the phytoplankton community along the French coast of the
937 eastern English Channel and the southern Bight of the North Sea. *Environ.*
938 *Soc.* 71, 821–833. <https://doi.org/10.4135/9781412953924.n678>
- 939 Hurrell, J.W., 1995. Decadal trends in the North Atlantic oscillation: Regional temperatures
940 and precipitation. *Science* (80-.). 269, 676–679.
941 <https://doi.org/10.1126/science.269.5224.676>
- 942 Hurrell, J.W., Deser, C., 2009. North Atlantic climate variability: The role of the North
943 Atlantic Oscillation. *J. Mar. Syst.* 78, 28–41.
944 <https://doi.org/10.1016/j.jmarsys.2008.11.026>
- 945 Idier, D., Castelle, B., Charles, E., Mallet, C., 2013. Longshore sediment flux hindcast:
946 spatio-temporal variability along the SW Atlantic coast of France. *J. Coast. Res.* 165,
947 1785–1790. <https://doi.org/10.2112/si65-302.1>
- 948 Ifremer, 2017. Bulletin de la Surveillance de la Qualité du Milieu Marin Littoral 2016.
949 Résultats acquis jusqu'en 2016. Ifremer/ODE/LITTORAL/LERAR/17.004. [http://](http://envlit.ifremer.fr/content/download/83308/602948/file/Bull_2017_AR.pdf)
950 envlit.ifremer.fr/content/download/83308/602948/file/Bull_2017_AR.pdfpp. 55.
951
- 952 Kaspar, H.F., Gillespie, P.A., Boyer, I.C., MacKenzie, A.L., 1985. Effects of mussel
953 aquaculture on the nitrogen cycle and benthic communities in Kenepuru Sound,
954 Marlborough Sounds, New Zealand. *Mar. Biol.* 85, 127–136.
955 <https://doi.org/10.1007/BF00397431>
- 956 Kolmogorov, A. (1933) Sulla determinazione empirica di una legge di distribuzione.
957 *Giornale dell'Istituto Italiano degli Attuari*, 4, 83-91.
958
- 959 Lerman, A., Mackenzie, F.T., Ver, L.M., 2004. Coupling of the perturbed C-N-P cycles in
960 industrial time. *Aquat. Geochemistry* 10, 3–32.
961 <https://doi.org/10.1023/B:AQUA.0000038955.73048.c1>
- 962 Lheureux, A., Savoye, N., Del Amo, Y., Goberville, E., Bozec, Y., Breton, E., Conan, P.,
963 L'Helguen, S., Mousseau, L., Raimbault, P., Rimelin-Maury, P., Seuront, L., Vuillemin,
964 R., Caparros, J., Cariou, T., Cordier, M., Corre, A., Costes, L., Crispi, O., Crouvoisier,

- 965 M., Crouvoisier, M., Derriennic, H., Devesa, J., Durozier, M., Ferreira, S., Garcia, N.,
 966 Grossteffan, E., Gueux, A., Lafont, M., Lagadec, V., Lecuyer, E., Leroux, C., Macé, E.,
 967 Maria, E., Mornet, L., Nowaczyk, A., Parra, M., Petit, F., David, V., 2021. Bi-decadal
 968 variability in physico-biogeochemical characteristics of temperate coastal ecosystems:
 969 from large-scale to local drivers. *Mar. Ecol. Prog. Ser.* 660, 19–35.
 970 <https://doi.org/10.3354/meps13577>
- 971 Liénart, C., Savoye, N., Bozec, Y., Breton, E., Conan, P., David, V., Feunteun, E.,
 972 Grangeré, K., Kerhervé, P., Lebreton, B., Lefebvre, S., L'Helguen, S., Mousseau, L.,
 973 Raimbault, P., Richard, P., Riera, P., Sauriau, P.G., Schaal, G., Aubert, F., Aubin, S.,
 974 Bichon, S., Boinet, C., Bourasseau, L., Bréret, M., Caparros, J., Cariou, T., Charlier,
 975 K., Claquin, P., Cornille, V., Corre, A.M., Costes, L., Crispi, O., Crouvoisier, M.,
 976 Czamanski, M., Del Amo, Y., Derriennic, H., Dindinaud, F., Durozier, M., Hanquiez, V.,
 977 Nowaczyk, A., Devesa, J., Ferreira, S., Fornier, M., Garcia, F., Garcia, N., Geslin, S.,
 978 Grossteffan, E., Gueux, A., Guillaudeau, J., Guillou, G., Joly, O., Lachaussée, N.,
 979 Lafont, M., Lamoureux, J., Lecuyer, E., Lehodey, J.P., Lemeille, D., Leroux, C., Macé,
 980 E., Maria, E., Pineau, P., Petit, F., Pujon-Pay, M., Rimelin-Maury, P., Sultan, E., 2017.
 981 Dynamics of particulate organic matter composition in coastal systems: A spatio-
 982 temporal study at multi-systems scale. *Prog. Oceanogr.* 156, 221–239.
 983 <https://doi.org/10.1016/j.pocean.2017.03.001>
- 984 Liénart, C., Savoye, N., David, V., Ramond, P., Rodriguez Tress, P., Hanquiez, V., Marieu,
 985 V., Aubert, F., Aubin, S., Bichon, S., Boinet, C., Bourasseau, L., Bozec, Y., Bréret, M.,
 986 Breton, E., Caparros, J., Cariou, T., Claquin, P., Conan, P., Corre, A.M., Costes, L.,
 987 Crouvoisier, M., Del Amo, Y., Derriennic, H., Dindinaud, F., Duran, R., Durozier, M.,
 988 Devesa, J., Ferreira, S., Feunteun, E., Garcia, N., Geslin, S., Grossteffan, E., Gueux,
 989 A., Guillaudeau, J., Guillou, G., Jolly, O., Lachaussée, N., Lafont, M., Lagadec, V.,
 990 Lamoureux, J., Lauga, B., Lebreton, B., Lecuyer, E., Lehodey, J.P., Leroux, C.,
 991 L'Helguen, S., Macé, E., Maria, E., Mousseau, L., Nowaczyk, A., Pineau, P., Petit, F.,
 992 Pujon-Pay, M., Raimbault, P., Rimmelin-Maury, P., Rouaud, V., Sauriau, P.G., Sultan,
 993 E., Susperregui, N., 2018. Dynamics of particulate organic matter composition in
 994 coastal systems: Forcing of spatio-temporal variability at multi-systems scale. *Prog.*
 995 *Oceanogr.* 162, 271–289. <https://doi.org/10.1016/j.pocean.2018.02.026>
- 996 Lindström Swanberg, I., 1991. The influence of the filter-feeding bivalve *Cerastoderma*
 997 *edule* L. on microphytobenthos: a laboratory study. *J. Exp. Mar. Bio. Ecol.* 151, 93–
 998 111. [https://doi.org/10.1016/0022-0981\(91\)90018-R](https://doi.org/10.1016/0022-0981(91)90018-R)
- 999 Lucas, C.H., Widdows, J., Brinsley, M.D., Salkeld, P.N., Herman, P.M.J., 2000. Benthic-
 1000 pelagic exchange of microalgae at a tidal flat. 1. Pigment analysis. *Mar. Ecol. Prog.*
 1001 *Ser.* 196, 59–73. <https://doi.org/10.3354/meps196059>
- 1002 Madsen, J.D., Chambers, P.A., James, W.F., Koch, E.W., Westlake, D.F., 2001. The
 1003 interaction between water movement, sediment dynamics and submersed
 1004 macrophytes. *Hydrobiologia* 444, 71–84. <https://doi.org/10.1023/A:1017520800568>
- 1005 Ménesguen, A., Piriou, J.Y., 1995. Nitrogen loadings and macroalgal (*Ulva* sp.) mass
 1006 accumulation in brittany (France). *Ophelia* 42, 227–237.
- 1007 Ménesguen, A., Piriou, J.Y., Dion, P., Auby, I., 1997. Les "marées vertes", un exemple
 1008 d'eutrophisation à macroalgues . In Dauvin, J.-C. (Ed.) (1997). Les biocénoses
 1009 marines et littorales françaises des côtes Atlantique, Manche et Mer du Nord:
 1010 synthèse, menaces et perspectives. Collection Patrimoines naturels: Série Patrimoine
 1011 écologique, 28. Muséum national d'Histoire naturelle: Paris. ISBN 2-86515-102-6.
 1012 chap.5.6, pp.212-217. (MNHN)

- 1013 Metson, G.S., Lin, J., Harrison, J.A., Compton, J.E., 2017. Linking terrestrial phosphorus
1014 inputs to riverine export across the United States. *Water Res.* 124, 177–191.
1015 <https://doi.org/10.1016/j.watres.2017.07.037>
- 1016 Nielsen, E., Richardson, K., 1996. Can changes in the fisheries yield in the Kattegat (1950-
1017 1992) be linked to changes in primary production? *ICES J. Mar. Sci.* 53, 988–994.
1018 <https://doi.org/10.1006/jmsc.1996.0123>
- 1019 Nixon, S.W., Oviatt, C.A., Frithsen, J., Sullivan, B., 1986. Nutrients and the productivity of
1020 estuarine and coastal marine ecosystems. *J. Limnol. Soc. South. Africa* 12, 43–71.
1021 <https://doi.org/10.1080/03779688.1986.9639398>
- 1022 Nowicki, B.L., Nixon, S.W., 1985. Benthic nutrient remineralization in a coastal lagoon
1023 ecosystem. *Estuaries* 8, 182–190. <https://doi.org/10.2307/1352199>
- 1024 Paerl, H.W., 2009. Controlling eutrophication along the freshwater-Marine continuum: Dual
1025 nutrient (N and P) reductions are essential. *Estuaries and Coasts* 32, 593–601.
1026 <https://doi.org/10.1007/s12237-009-9158-8>
- 1027 Papush, L., Danielsson, Å., 2006. Silicon in the marine environment: Dissolved silica
1028 trends in the Baltic Sea. *Estuar. Coast. Shelf Sci.* 67, 53–66.
1029 <https://doi.org/10.1016/j.ecss.2005.09.017>
- 1030 Peng, S., Qin, X., Shi, H., Zhou, R., Dai, M., Ding, D., 2012. Distribution and controlling
1031 factors of phytoplankton assemblages in a semi-enclosed bay during spring and
1032 summer. *Mar. Pollut. Bull.* 64, 941–948.
1033 <https://doi.org/10.1016/j.marpolbul.2012.03.004>
- 1034 Petris, G., 2010. An R package for dynamic linear models. *J. Stat. Softw.* 36, 1–16.
1035 <https://doi.org/10.18637/jss.v036.i12>
- 1036 Plus, M., Auby, I., Maurer, D., Trut, G., Del Amo, Y., Dumas, F., Thouvenin, B., 2015.
1037 Phytoplankton versus macrophyte contribution to primary production and
1038 biogeochemical cycles of a coastal mesotidal system. A modelling approach. *Estuar.
1039 Coast. Shelf Sci.* 165, 52–60. <https://doi.org/10.1016/j.ecss.2015.09.003>
- 1040 Plus, M., Dalloyau, S., Trut, G., Auby, I., de Montaudouin, X., Emery, E., Noël, C., Viala, C.,
1041 2010. Long-term evolution (1988-2008) of *Zostera* spp. meadows in Arcachon Bay
1042 (Bay of Biscay). *Estuar. Coast. Shelf Sci.* 87, 357–366.
1043 <https://doi.org/10.1016/j.ecss.2010.01.016>
- 1044 Plus, M., Dumas, F., Stanisière, J.Y., Maurer, D., 2009. Hydrodynamic characterization of
1045 the Arcachon Bay, using model-derived descriptors. *Cont. Shelf Res.* 29, 1008–1013.
1046 <https://doi.org/10.1016/j.csr.2008.12.016>
- 1047 R Development Core Team: R: A Language and Environment for Statistical
1048 Computing. R Foundation for Statistical Computing, Vienna, Austria, available
1049 at: [https://www.R-](https://www.R-project.org/) project.org/ (last access: 15 May 2021), 2021.
1050
- 1051 Ragueneau, O., Conley, D.J., Leynaert, A., Longphuir, S.N., Slomp, C.P., 2006.
1052 Responses of coastal ecosystems to anthropogenic perturbations of silicon cycling, in:
1053 V. Ittekkot, D. Unger, C. Humborg, & N.A.A. (Ed.), *The Silicon Cycle - Human
1054 Perturbations and Impacts on Aquatic Systems*. Washington: Island press, pp. 197–
1055 213.

- 1056 Ribaudo, C., Plus, M., Ganthu, F., Auby, I., 2016. Carbon sequestration loss following
1057 *Zostera noltei* decline in the Arcachon Bay (France). *Estuar. Coast. Shelf Sci.* 179, 4–
1058 11. <http://dx.doi.org/10.1016/j.ecss.2016.01.024>
- 1059 Ricciardi, A., Bourget, E., 1998. Weight-to-weight conversion factors for marine benthic
1060 macroinvertebrates. *Mar. Ecol. Prog. Ser.* 163, 245–251.
1061 <https://doi.org/10.3354/meps163245>
- 1062 Rimmelin, P., Dumon, J.C., Maneux, E., Gonçalves, A., 1998. Study of annual and
1063 seasonal dissolved inorganic nitrogen inputs into the Arcachon Lagoon, Atlantic Coast
1064 (France). *Estuar. Coast. Shelf Sci.* 47, 649–659.
1065 <https://doi.org/10.1006/ecss.1998.0384>
- 1066 Robert, R., Guillocheau, N., Collos, Y., 1987. Hydrobiological parameters during an annual
1067 cycle in the Arcachon Basin. *Mar. Biol.* 95, 631–640.
1068 <https://doi.org/10.1007/BF00393107>
- 1069 Romero, E., Le Gendre, R., Garnier, J., Billen, G., Fisson, C., Silvestre, M., Riou, P., 2016.
1070 Long-term water quality in the lower Seine: Lessons learned over 4 decades of
1071 monitoring. *Environ. Sci. Policy* 58, 141–154.
1072 <https://doi.org/10.1016/j.envsci.2016.01.016>
- 1073 Roser, M. and Ritchie, H., (2013). Fertilizers. Published online at OurWorldInData.org.
1074 Retrieved from: '<https://ourworldindata.org/fertilizers>' [Online Resource] Accessed
1075 22nd January 2021
- 1076 Saeck, E.A., O'Brien, K.R., Weber, T.R., Burford, M.A., 2013. Changes to chronic
1077 nitrogen loading from sewage discharges modify standing stocks of coastal
1078 phytoplankton. *Mar. Pollut. Bull.* 71, 159–167.
1079 <https://doi.org/10.1016/j.marpolbul.2013.03.020>
- 1080 Sanchez, F., Caill-Milly, N., Lissardy, M., 2018. Campagne d'évaluation du stock de
1081 palourdes du bassin d'Arcachon - Année 2018. Rapport Ifremer
1082 R.ODE/LITTORAL/LER AR 18.015, 61 p.
1083
- 1084 Sanchez, G., 2013. PLS Path Modeling with R. *R Packag. Notes* 235.
1085 <https://doi.org/citeulike-article-id:13341888>
- 1086 Sand-Jensen, K., Bruun, H.H., Bastrup-Spohr, L., 2017. Decade-long time delays in
1087 nutrient and plant species dynamics during eutrophication and re-oligotrophication of
1088 Lake Fure 1900–2015. *J Ecol* 105, 690–700. <https://doi.org/10.1111/1365-2745.12715>.
- 1089 Scourzic T., Loyen M., Fabre E., Tessier A. Dalias N., Trut G., Maurer D. et
1090 Simonnet B., 2011. Evaluation du stock d'huîtres sauvages et en élevage dans le
1091 Bassin d'Arcachon. Contrat Agence des Aires Marines Protégées &
1092 OCEANIDE, Fr : 70
1093
- 1094 Seitzinger, S.P., Kroeze, C., Bouwman, A.F., Caraco, N., Dentener, F., Styles, R. V., 2002.
1095 Global patterns of dissolved inorganic and particulate nitrogen inputs to coastal
1096 systems: Recent conditions and future projections. *Estuaries* 25, 640–655.
1097 <https://doi.org/10.1007/BF02804897>
- 1098 Scheffer M; Carpenter S.R. 2003. Catastrophic regime shifts in ecosystems: linking theory
1099 to observation. *Trends Ecol Evol* 18:648–656. doi:10.1016/j.tree.2003.09.002

- 1100 Scheffer M., Bascompte J., Brock W.A., Brovkin V., Carpenter, S.R., Dakos, V., Held, H.,
1101 van Nes, E.H., Rietkerk, M., Sugihara, G. 2009. Early-warning signals for critical
1102 transitions. *Nature* 461:53–59. doi:10.1038/nature08227
- 1103 Sfriso, A., Buosi, A., Mistri, M., Munari, C., Franzoi, P., Sfriso, A.A., 2019. Long-term
1104 changes of the trophic status in transitional ecosystems of the northern Adriatic Sea,
1105 key parameters and future expectations: The lagoon of Venice as a study case. *Nat.*
1106 *Conserv.* 34, 193–215. <https://doi.org/10.3897/natureconservation.34.30473>
- 1107 Sinha, E., Michalak, A.M., Balaji, V., 2017. Eutrophication will increase during the 21st
1108 century as a result of precipitation changes. *Science* (80-.). 357, 1–5.
1109 <https://doi.org/10.1126/science.aan2409>
- 1110 Stoffer, D.S., Toloj, C.M.C., 1992. A note on the Ljung-Box-Pierce portmanteau statistic
1111 with missing data. *Stat. Probab. Lett.* 13, 391–396.
- 1112 Taylor, D.I., Oviatt, C.A., Giblin, A.E., Tucker, J., Diaz, R.J., Keay, K., 2020. Wastewater
1113 input reductions reverse historic hypereutrophication of Boston Harbor, USA. *Ambio*
1114 49, 187–196. <https://doi.org/10.1007/s13280-019-01174-1>
- 1115 Tréguer, P., Nelson, D.M., Van Bennekom, A.J., Demaster, D.J., Leynaert, A., Quéguiner,
1116 B., 1995. The silica balance in the world ocean: A reestimate. *Science* (80-.). 268,
1117 375–379. <https://doi.org/10.1126/science.268.5209.375>
- 1118 United Nations, Department of Economic and Social Affairs, Population Division 2019.
1119 World Population Prospects 2019, custom data acquired via website. Accessed 22nd
1120 January 2021
- 1121 Wainright, S., 1990. Sediment-to-water fluxes of particulate material and microbes by
1122 resuspension and their contribution to the planktonic food web. *Mar. Ecol. Prog. Ser.*
1123 62, 271–281. <https://doi.org/10.3354/meps062271>
- 1124 Ward, L.G., Michael Kemp, W., Boynton, W.R., 1984. The influence of waves and
1125 seagrass communities on suspended particulates in an estuarine embayment. *Mar.*
1126 *Geol.* 59, 85–103. [https://doi.org/10.1016/0025-3227\(84\)90089-6](https://doi.org/10.1016/0025-3227(84)90089-6)
- 1127 Wasserman, J.-C., Dumon, J.-C., Latouche, C., 1992. Bilan de 18 éléments-trace et de 7
1128 éléments majeurs dans un environnement peuplé de zostères *Zostera noltei*. *Vie*
1129 *milieu* 42, 15–20.
- 1130 West, M., Harrison, J., 1997. Bayesian Forecasting & Dynamic Models, Springer S. ed.
1131 Springer-Verlag New York, Inc., 175 Fifth Avenue, New York, NY 10010, USA, New-
1132 York.
- 1133 Xenopoulos, M.A., Downing, J.A., Kumar, M.D., Menden-Deuer, S., Voss, M., 2017.
1134 Headwaters to oceans: Ecological and biogeochemical contrasts across the aquatic
1135 continuum. *Limnol. Oceanogr.* 62, S3–S14. <https://doi.org/10.1002/lno.10721>
- 1136 Yue, S., Wang, C.Y., 2004. The Mann-Kendall test modified by effective sample size to
1137 detect trend in serially correlated hydrological series. *Water Resour. Manag.* 18, 201–
1138 218. <https://doi.org/10.1023/B:WARM.0000043140.61082.60>
- 1139 Zhang, J.Z., Huang, X.L., 2011. Effect of temperature and salinity on phosphate sorption
1140 on marine sediments. *Environ. Sci. Technol.* 45, 6831–6837.
1141 <https://doi.org/10.1021/es200867p>
- 1142 Zhang, Q., Fisher, T.R., Trentacoste, E.M., Buchanan, C., Gustafson, A.B., Karrh, R.,
1143 Murphy, R.R., Keisman, J., Wu, C., Tian, R., Testa, J.M., Tango, P.J., 2021. Nutrient
1144 limitation of phytoplankton in Chesapeake Bay: Development of an empirical approach

1145 for water-quality management. Water Res. 188, 166407.
1146 <https://doi.org/10.1016/j.watres.2020.116407>

